Energy momentum tensor and the D term in the bag model

Matt J. Neubelt, Andrew Sampino, Jonathan Hudson, Kemal Tezgin, and Peter Schweitzer

Departement of Physics, University of Connecticut, Storrs, Connecticut 06269, USA

The energy momentum tensor (EMT) form factors pave new ways for exploring hadron structure. Especially, the D-term related to the EMT form factor $D(t)$ has received a lot of attention due to its attractive physical interpretation in terms of mechanical properties. We study the nucleon EMT form factors and the associated densities in the bag model which we formulate for an arbitrary number of colors N_c and show that the EMT form factors are consistently described in this model in the large-N_c limit. The simplicity of the model allows us to test in a lucid way many theoretical concepts related to EMT form factors and densities including recently introduced concepts like normal and tangential forces, or monopole and quadrupole contributions to the angular momentum distribution. We also study the D-terms of the ρ-meson, Roper resonance, other N^* states, and Δ-resonances. Among the most interesting outcomes is the lucid demonstration of the deeper connection of EMT conservation, stability, the virial theorem, and the negative sign of the D-term.

I. INTRODUCTION

The perspective to access the hadronic energy momentum tensor (EMT) form factors [1] through studies of generalized parton distribution functions (GPDs) [2] in hard exclusive reactions [3–7] and their attractive interpretation in terms of mechanical properties [8] have attracted lots of interest in recent literature; see the review [9]. EMT form factors were studied in models [10–41], chiral perturbation theory [42–44], the meson-dominance approach [45], dispersion relations [46], lattice QCD [47–50], QCD light cone sum rules [51], and for photons [52,53]. Especially, the form factor $D(t)$ [54,55] gained increased attention due to its interpretation in terms of internal forces [8] spurred by recent attempts to extract phenomenological information on $D(t)$ [56–58].

In this work, we present a study of EMT properties in one of the simplest hadronic models: the bag model [59–61]. This model was introduced more than 40 years ago, but is still in use and continues giving helpful contributions to the understanding of hadron structure. In fact, the bag model has been used as an exploratory theoretical framework in many instances, often being the first model (or one of the first models) where newly introduced hadronic properties were investigated, including studies of nucleon structure functions [62,63], transversity

and other chiral-odd parton distribution functions [64], transverse momentum–dependent parton distributions [65–67], or double parton distribution functions [68,69]. The bag model was also the first model where GPDs and EMT form factors were studied [10].

In the present study, we will extend the work of Ref. [10] in multiple respects and investigate within this model concepts which appeared only after Ref. [10]. This includes the EMT densities introduced in Ref. [8] and further developed in Refs. [9] and [70–77]. The bag model provides an attractive theoretical framework for that. The version of the bag model used in this work is at variance with chiral symmetry which is a drawback. This model has, however, also important advantages: it is a consistent theoretical framework. Its simplicity allows one to obtain lucid insights which are more difficult to deduce from more complex models. Our results will help to improve the understanding of the nucleon structure and the EMT densities. The layout of our study is as follows.

After defining the EMT form factors and densities in Sec. II, we briefly introduce the bag model in Sec. III and study the quark EMT form factors in Sec. IV using a formulation of the model for a large number of colors N_c. The large-N_c limit will allow us to avoid technical problems associated with the evaluation of form factors in so-called independent-particle models like the bag model. We will use the large-N_c limit as a tool to derive consistent model expressions, and show that the $1/N_c$-corrections to the form factors are relatively small for small momentum transfers. In addition, the large-N_c limit provides a rigorous justification for the concept of three-dimensional (3D) densities which are studied in detail in

034013-1

Sec. V. We will evaluate the "gluonic" form factor $\bar{c}^G(t)$ due to the bag, which can only be computed by taking advantage of the EMT density formalism, and we will rigorously prove the internal consistency of the description. Section VI presents an extensive study of the D-term for the nucleon and other hadronic states including $N^\star$ states, ρ-mesons, and the Δ-resonances. We also include an insightful study of hypothetical highly excited bag model states. This is the only study of EMT properties of excited states available in the literature besides Q-balls [35], and we make the interesting observation that in both systems asymptotically the D-term grows as $D = -\text{const} \times M^{8/3}$ with the mass M of the excitation, even though the excited states have much different internal structures in the two frameworks. Section VII is dedicated to studies of limiting cases like the heavy quark limit, the large bag-radius limit, and the nonrelativistic limit of the nucleon, and discuss the behavior of the D-term in these limits. Our study is complemented by an instructive discussion in Sec. VIII of the D-term in a predecessor of the bag model [78], the Bogoliubov model [79], which is a counterexample where the nucleon is not fully consistently described. As a consequence, one finds an unphysical (positive) D-term in this model. This example also illustrates the necessity to study the complete EMT structure. The conclusions are presented in Sec. IX, and technical details can be found in Appendix. Some of our results were previously mentioned in Refs. [80,81].

II. EMT FORM FACTORS

The EMT form factors [1] can be defined in QCD in the following way,

$$
\langle p'|\hat{T}^a_{\mu\nu}(0)|p\rangle
$$
$$
= \bar{u}(p')\left[A^a(t)\frac{P_\mu P_\nu}{M_N} + J^a(t)\frac{i(P_\mu\sigma_{\nu\rho} + P_\nu\sigma_{\mu\rho})\Delta^\rho}{2M_N}\right.
$$
$$
\left. + D^a(t)\frac{\Delta_\mu\Delta_\nu - g_{\mu\nu}\Delta^2}{4M_N} + \bar{c}^a(t)M_N g_{\mu\nu}\right]u(p), \quad (1)
$$

where the kinematic variables are defined as

$$
P = \frac{1}{2}(p + p'), \qquad \Delta = (p' - p), \qquad t = \Delta^2. \quad (2)
$$

The EMT form factors for different partons $a = g, u, d, \ldots$ depend on renormalization scale μ, e.g., $A^a(t) = A^a(t, \mu^2)$, which we do not always indicate for brevity. The total EMT form factors $A(t) = \sum_a A^a(t, \mu^2)$ and analog for $J(t), D(t)$ are renormalization scale independent. The appearance of the form factors $\bar{c}^a(t, \mu^2)$ signals that the separate quark and gluon EMTs are not conserved. Only the total EMT is conserved, and consequently $\sum_a \bar{c}^a(t, \mu^2) = 0$.

The form factors of the EMT in Eq. (1) can be interpreted [8] in analogy to the electromagnetic form factors [82] in the Breit frame where $\Delta^0 = 0$. In the Breit frame, one can define the static energy momentum tensor as

$$
T_{\mu\nu}(\vec{r}, \vec{s}) = \int \frac{d^3\Delta}{2E(2\pi)^3}\exp(-i\vec{\Delta}\vec{r})\langle p', S'|\hat{T}_{\mu\nu}(0)|p, S\rangle \quad (3)
$$

with initial and final nucleon polarizations S and S' defined such that they are equal to $(0, \vec{s})$ in the respective rest frames, where the unit vector $\vec{s}$ denotes the quantization axis for the nucleon spin. This interpretation is subject to "relativistic corrections" as in the case of electromagnetic form factors [8,82] and is exact in the large-N_c limit [9].

The component $T_{00}(\vec{r})$ describes the energy density, and the components $T_{ik}(\vec{r})$ characterize the spatial distributions of forces experienced by the partons [8]. Both are independent of the polarization vector. The components $T_{0k}(\vec{r}, \vec{s})$ are related to the distributions of angular momentum. At $t = 0$, the form factors satisfy the constraints

$$
A(0) = \frac{1}{M_N}\int d^3r\, T_{00}(\vec{r}) = 1,
$$
$$
J(0) = \int d^3r\, \epsilon^{ijk}s_i r_j T_{0k}(\vec{r}, \vec{s}) = \frac{1}{2},
$$
$$
D(0) = -\frac{2M_N}{5}\int d^3r\, T_{ij}(\vec{r})\left(r^i r^j - \frac{\vec{r}^2}{3}\delta^{ij}\right) \equiv D. \quad (4)
$$

The constraints on $A(0)$ and $J(0)$ can be traced back to the fact that the EMT matrix elements contain information on the particle's mass and spin and are dictated by the transformation properties of the states [83,84]. The value of the form factor $D(t)$ at $t = 0$ is not constrained by any general principle. The components $T_{ij}(\vec{r})$ of the static stress tensor encode the information on the distribution of pressure and shear forces [8]

$$
T_{ij}(\vec{r}) = s(r)\left(\frac{r_i r_j}{r^2} - \frac{1}{3}\delta_{ij}\right) + p(r)\delta_{ij}. \quad (5)
$$

Here, $p(r)$ describes the radial distribution of the pressure inside the hadron, and $s(r)$ is the distribution of shear forces [8]. Both functions are related to each other due to the EMT conservation by the differential equation

$$
\frac{2}{3}\frac{\partial s(r)}{\partial r} + \frac{2s(r)}{r} + \frac{\partial p(r)}{\partial r} = 0. \quad (6)
$$

The conservation of the EMT also provides two equivalent expressions for the D-term in terms of $p(r)$ or $s(r)$ as

$$
D = -\frac{4}{15}M_N\int d^3r\, r^2 s(r) = M_N\int d^3r\, r^2 p(r). \quad (7)
$$

Further properties of EMT densities will be discussed below.

III. BAG MODEL

In the bag model, one describes baryons (mesons) by placing $N_c = 3$ noninteracting quarks (a $\bar{q}q$ pair) in a color-singlet state inside a "bag." In its rest frame, the bag is a spherical region of radius R carrying the energy density $B > 0$ [59]. The Lagrangian of the bag model can be written as [78]

$$\mathcal{L} = \mathcal{L}_Q + \mathcal{L}_{\text{surf}} + \mathcal{L}_G,$$

$$\mathcal{L}_Q = \sum_q \left[\bar{\psi}_q \left(-\frac{i}{2} \overleftarrow{\slashed{\partial}} + \frac{i}{2} \overrightarrow{\slashed{\partial}} - m \right) \psi_q \right] \Theta_V,$$

$$\mathcal{L}_{\text{surf}} = \frac{1}{2} \sum_q \bar{\psi}_q \psi_q \eta^\mu \partial_\mu \Theta_V, \qquad \mathcal{L}_G = -B\Theta_V \qquad (8)$$

with the following definitions referring to the rest frame of the bag:

$$\Theta_V = \Theta(R - r), \qquad \delta_S = \delta(R - r),$$
$$\eta^\mu = (0, \vec{e}_r), \qquad \vec{e}_r = \vec{r}/r, \qquad r = |\vec{r}|. \qquad (9)$$

In Eq. (8), we defined for later convenience the contributions of quarks $\mathcal{L}_Q$, "gluons" $\mathcal{L}_G$, and the interaction $\mathcal{L}_{\text{surf}}$ with the bag surface. We deal with a very crude model of confinement, so the contribution of gluons should not be understood literally. It "resembles" the QCD gluon contribution remotely in the sense that (i) it cannot be expressed in terms of fermionic degrees of freedom and (ii) is crucial for the formation of bound states in this model. In fact, if we let $R \to \infty$, then $\Theta_V \to 1$, $\partial_\mu \Theta_V \to 0$, and we recover free and unbound quarks. The Euler-Lagrange equations of the theory (8) are given by

$$(i\slashed{\partial} - m)\psi_q = 0 \quad \text{for } r < R \quad \text{(free quarks)}, \qquad (10a)$$

$$i\slashed{\eta}\psi_q = \psi_q \quad \text{for } \vec{r} \in S \quad \text{(linear boundary condition)}, \qquad (10b)$$

$$-\frac{1}{2} \sum_q \eta_\mu \partial^\mu \bar{\psi}_q \psi_q = B \quad \text{for } \vec{r} \in S$$

$$\text{(non-linear boundary condition).} \qquad (10c)$$

The boundary conditions (10b) and (10c) are equivalent to the statement that there is no energy momentum flow out of the bag, i.e., $\eta_\mu T^{\mu\nu}(t, \vec{r}) = 0$ for $\vec{r} \in S$ [59], which provides a simple model of confinement.

In the positive parity sector, which contains the ground state, the wave functions are given by

$$\psi_s(t, \vec{r}) = e^{-i\varepsilon_i t} \phi_s(\vec{r}),$$

$$\phi_s(\vec{r}) = \frac{A}{\sqrt{4\pi}} \begin{pmatrix} \alpha_+ j_0(\omega_i r/R)\chi_s \\ \alpha_- j_1(\omega_i r/R)i\vec{\sigma}\vec{e}_r\chi_s \end{pmatrix},$$

$$A = \left(\frac{\Omega_i(\Omega_i - mR)}{R^3 j_0^2(\omega_i)(2\Omega_i(\Omega_i - 1) + mR)} \right)^{1/2}, \qquad (11)$$

where $\alpha_\pm = \sqrt{1 \pm mR/\Omega_i}$ with $\Omega_i = \sqrt{\omega_i^2 + m^2 R^2}$. The σ^i are 2×2 Pauli matrices, and χ_s are two-component Pauli spinors. The spherical Bessel functions are defined in Appendix. The single-quark energies are given by $\varepsilon_i = \Omega_i/R$ where the ω_i denote solutions of the transcendental equation

$$\omega_i = (1 - mR - \Omega_i) \tan \omega_i, \qquad (12)$$

the lowest (ground state) solution of which is $\omega_0 \approx 2.04$ for massless quarks. If mR is varied from 0 to infinity, the ground state solution $\omega_0 = \omega_0(mR)$ covers the interval

$$2.04 \lesssim \omega_0(mR) \leq \pi. \qquad (13)$$

The momentum space wave functions are defined by the Fourier transform $\varphi_s(\vec{k}) = \int d^3 r e^{-i\vec{k}\vec{r}} \phi_s(\vec{r})$ and given by

$$\varphi_s(\vec{k}) = \sqrt{4\pi}AR^3 \begin{pmatrix} \alpha_+ t_0(k)\chi_s \\ \alpha_- t_1(k)\vec{\sigma}\vec{e}_k\chi_s \end{pmatrix}, \qquad (14)$$

where $\vec{e}_k = \vec{k}/k$ with $k = |\vec{k}|$. The functions $t_l(k)$ for $l = 0, 1$ are given by

$$t_l(k) = \int_0^1 du u^2 j_l(ukR) j_l(u\omega_i). \qquad (15)$$

The constant A in Eqs. (11) and (14) ensures the normalization

$$\int d^3 r \phi_{s'}^\dagger(\vec{r})\phi_s(\vec{r}) = \int \frac{d^3 k}{(2\pi)^3} \varphi_{s'}^\dagger(\vec{k})\varphi_s(\vec{k}) = \delta_{s's}. \qquad (16)$$

The nucleon wave functions with definite spin-isospin quantum numbers are constructed from the single-quark wave functions (11) assuming SU(4) spin-flavor symmetry. We will not need the explicit expressions here, and only quote the resulting SU(4) spin-flavor factors which appear in respectively spin-independent (N_q) and spin-dependent (P_q) matrix elements for a proton made of N_c quarks (for neutron interchange $u \leftrightarrow d$) [85]

$$N_u = \frac{N_c + 1}{2}, \qquad N_d = \frac{N_c - 1}{2}, \qquad (17a)$$

$$P_u = \frac{N_c + 5}{6}, \qquad P_d = \frac{-N_c + 1}{6}. \qquad (17b)$$

For the proton and $N_c = 3$, the familiar values $N_u = 2$, $N_d = 1$, $P_u = \frac{4}{3}$, and $P_d = -\frac{1}{3}$ are reproduced.

IV. EMT FORM FACTORS OF QUARKS

In this section, we compute the matrix elements of the quark EMT $T_Q^{\mu\nu}$ in the limit of a large number of colors N_c, check the consistency of the results, discuss the role of $1/N_c$ corrections, and compare to results from literature.

A. Kinematics and scaling of EMT form factors in large-N_c limit

In this limit, the nucleon mass behaves as $M_N = \mathcal{O}(N_c)$. This means the nucleon is a heavy particle, and its motion is nonrelativistic, i.e., the nucleon energies E and E' are given by $M_N + \mathcal{O}(N_c^{-1})$, while the nucleon momenta $\vec{p}$ and $\vec{p}'$ are of the order $\mathcal{O}(N_c^0)$. For the kinematic variables (2), this implies

$$P^0 = \mathcal{O}(N_c), \quad \vec{P} = \mathcal{O}(N_c^0), \quad \vec{\Delta} = \mathcal{O}(N_c^0), \quad \Delta^0 = \mathcal{O}(N_c^{-1}).$$

$$(18)$$

Thus, $P^\mu = (M_N, 0, 0, 0)$ and $\Delta^\mu = (0, \vec{\Delta})$ and $t = -\vec{\Delta}^2$ modulo $1/N_c$ corrections. Notice that the nonrelativistic motion concerns only the nucleon. The motion of the quarks inside the nucleon can still be ultrarelativistic for light or massless quarks. In the large-N_c limit, the bag model is still a relativistic model. Only if in addition to the large-N_c limit one also would choose to make the quarks heavy would one recover the picture of a nonrelativistic quark model (which we shall explore in Sec. VII).

In order to evaluate the expressions for the EMT form factors (1), we also have to take into account the large-N_c behavior of the quark EMT form factors [6]

$$A^Q(t) = \mathcal{O}(N_c^0), \qquad J^Q(t) = \mathcal{O}(N_c^0),$$
$$D^Q(t) = \mathcal{O}(N_c^2), \qquad \bar{c}^Q(t) = \mathcal{O}(N_c^0). \qquad (19)$$

Notice that the index Q denotes the isoscalar $(u + d)$ flavor combinations. The isovector $(u - d)$ flavor combinations have different N_c scalings: $A^{u-d}(t) = \mathcal{O}(N_c^{-1})$, $J^{u-d}(t) = \mathcal{O}(N_c)$, $D^{u-d}(t) = \mathcal{O}(N_c)$, and $\bar{c}^{u-d}(t) = \mathcal{O}(N_c^{-1})$ [6].

B. Form factors of the symmetric quark EMT in bag model

In the large-N_c limit, i.e., considering Eqs. (18) and (19), the expressions for the EMT form factors (1) become

$$\langle p', s' | \hat{T}_Q^{00}(0) | p, s \rangle$$
$$= 2M_N^2 \left[A^Q(t) - \frac{t}{4M_N^2} D^Q(t) + \bar{c}^Q(t) \right] \delta_{ss'} \qquad (20a)$$

$$\langle p', s' | \hat{T}_Q^{ik}(0) | p, s \rangle$$
$$= 2M_N^2 \left[D^Q(t) \frac{\Delta^i \Delta^k - \delta^{ik} \vec{\Delta}^2}{4M_N^2} - \bar{c}^Q(t) \delta^{ik} \right] \delta_{ss'} \qquad (20b)$$

$$\langle p', s' | \hat{T}_Q^{0k}(0) | p, s \rangle = 2M_N^2 \left[J^Q(t) \frac{(-i\vec{\Delta} \times \vec{\sigma}_{s's})^k}{2M_N} \right], \qquad (20c)$$

where we used $\chi_{s'}^\dagger \chi_s = \delta_{ss'}$ and defined $\vec{\sigma}_{s's} = \chi_{s'}^\dagger \vec{\sigma} \chi_s$. The generic expression to evaluate nucleon matrix elements of quark bilinear operators of the type $\bar{\Psi}_q \hat{O} \Psi_q$ in the bag model in the large-N_c limit is given by

$$\langle N(p', s') | \bar{\Psi}_q \hat{O} \Psi_q | N(p, s) \rangle = 2M_N \int \frac{d^3k}{(2\pi)^3} \bar{\varphi}_{s'}(\vec{k}') \hat{O} \varphi_s(\vec{k}),$$
$$\vec{k}' = \vec{k} + \vec{\Delta}. \qquad (21)$$

The prefactor $2M_N$ originates in the large-N_c limit from the factor $2P^0$ in the covariant normalization of the nucleon states. The symmetric quark EMT is given by (the arrows indicate which wave functions are differentiated)

$$T_q^{\mu\nu} = \frac{1}{4} \bar{\psi}_q (-i\overleftarrow{\partial}^\mu \gamma^\nu - i\overleftarrow{\partial}^\nu \gamma^\mu + i\overrightarrow{\partial}^\mu \gamma^\nu + i\overrightarrow{\partial}^\nu \gamma^\mu) \psi_q. \qquad (22)$$

In order to perform the calculations, we choose $\vec{\Delta} = (0, 0, \Delta^3)$ and the nucleon polarization along the z-axis. We define $k_\perp^2 = k_1^2 + k_2^2$, $k = |\vec{k}|$, $k' = |\vec{k}'|$ with $\vec{k}' = \vec{k} + \vec{\Delta} = (k^1, k^2, k^3 + \Delta^3)$ in our frame. The results read

$$A^Q(t) - \frac{t}{4M_N^2} D^Q(t) + \bar{c}^Q(t) = \frac{4\pi A^2 R^6 N_c}{M_N} \int \frac{d^3k}{(2\pi)^3} \varepsilon_0 [\alpha_+^2 t_0(k) t_0(k') + \alpha_-^2 \vec{e}_k \vec{e}_{k'} t_1(k) t_1(k')], \qquad (23a)$$

$$\frac{t}{4M_N^2} D^Q(t) - \bar{c}^Q(t) = \frac{4\pi A^2 R^6 N_c}{M_N} \int \frac{d^3k}{(2\pi)^3} \alpha_+ \alpha_- \frac{k_\perp^2}{2} \left[t_0(k) t_1(k') \frac{1}{k'} + t_0(k') t_1(k) \frac{1}{k} \right], \qquad (23b)$$

$$-\bar{c}^Q(t) = \frac{4\pi A^2 R^6 N_c}{M_N} \int \frac{d^3k}{(2\pi)^3} \alpha_+ \alpha_- \frac{(k'^3 + k^3)}{2} \left[t_0(k) t_1(k') \frac{k'^3}{k'} + t_0(k') t_1(k) \frac{k^3}{k} \right], \qquad (23c)$$

$$J^Q(t) = 4\pi A^2 R^6 \int \frac{\mathrm{d}^3 k}{(2\pi)^3} \left[\alpha_+ \alpha_- \frac{\varepsilon_0}{\Delta^3} \left(-t_0(k')t_1(k)\frac{k^3}{k} + t_0(k)t_1(k')\frac{k'^3}{k'} \right) + \frac{k_\perp^2}{2}\alpha_-^2 \frac{t_1(k)}{k}\frac{t_1(k')}{k'} \right].$$ (23d)

Hereby, Eq. (23a) follows from T_Q^{00} in (20a), Eq. (23b) follows from T_Q^{11} or T_Q^{22} in (20b), Eq. (23c) is obtained from T_Q^{33} in (20b), and Eq. (23d) follows from T_Q^{01} or T_Q^{02} in (20c), while T_Q^{03} vanishes. The canonical EMT has a symmetric part which coincides with what we discussed above and an antisymmetric part which is discussed in Appendix.

C. Numerical results

Evaluating Eqs. (23a)–(23d) for massless quarks yields the curves shown in Fig. 1 as solid lines. These results refer to the leading order in the large-N_c limit and are consequently valid for $|t| \ll M_N^2$. The obtained form factors satisfy the general requirements at $t = 0$ namely $A^Q(0) = 1$ and $J^Q(0) = \frac{1}{2}$. Furthermore, it is $\bar{c}^Q(0) = -\frac{1}{4}$ which is a bag model specific result [10]. All three constraints can be proven analytically, but the proofs are lengthy, not enlightening, and we do not show them. The D-term is not fixed by any general constraint. It assumes the value $D^Q(0) = -1.145$ for massless quarks. We will discuss the D-term in more detail below in Sec. VI.

The results $A^Q(0) = 1$ and $J^Q(0) = \frac{1}{2}$ mean that quarks carry 100% of the momentum and spin of the nucleon. The appearance of the form factor $\bar{c}^Q(t) \neq 0$ means, however, that the quark part of the EMT, $T_{\mu\nu}^Q$, is not conserved. To have a conserved total EMT, one must include also nonfermionic contributions associated with the bag, i.e., "gluonic contributions" in the sense explained in Sec. III. At this point, it is not clear how to formulate a wave function of the bag and compute the gluonic EMT form factors in the bag model, but in Sec. V, we will see that this can be naturally achieved by taking advantage of the concept of 3D spatial EMT densities.

D. $1/N_c$ corrections

The large-N_c results are theoretically consistent, which is crucial for our study. However, it is instructive to get insights on the size of $1/N_c$-corrections by comparing our results with those of Ref. [10] obtained for finite N_c. We can distinguish different types of $1/N_c$-corrections. If we do not implement the kinematic effects (18) and large-N_c counting rules (19), we recover the "no-boost results" by Ji *et al.* from Ref. [10]. This type of $1/N_c$-correction only affects the form factor $A(t)$ where it has a small effect for $|t|$ below 1 GeV²; see the curve depicted by the dotted line in comparison to the solid line in Fig. 1(a). The form factors $J^Q(t)$, $D^Q(t)$, and $\bar{c}^Q(t)$ are not affected by these corrections, so the no-boost results from Ref. [10] (dotted lines) coincide with our large-N_c results (solid lines) in Figs. 1(b)–1(d).

A conceptually different type of corrections arises because for finite N_c it is necessary to take into account relativistic corrections associated with boosting the quark wave function (14) to a frame where the nucleon moves with velocity $\vec{v}$: $\psi(t, \vec{x}) \rightarrow S(\Lambda_{\vec{v}})\psi(t', \vec{x}')$ with $S(\Lambda) = \exp(w\gamma^0\gamma^3)$ where $\Lambda_{\vec{v}}$ is the Lorentz transformation for a boost along the z-axis with $\vec{v} = (0, 0, \tanh(w))$ where $\sinh(w) = |\vec{\Delta}|/(2M_N)$ [10]. The results obtained in this way are depicted as dashed lines in Fig. 1. The constraint $J^Q(0) = \frac{1}{2}$ is no longer satisfied, see Fig. 1(b), because "the boosted bag wave function does not have the correct Lorentz symmetry" [10]. This artifact can in principle be avoided using Peierls-Yoccoz projections [86] or center-of-mass freedom separation methods [87], which were not performed in Ref. [10]. For our purposes, it is completely sufficient to observe that in practice such boost effects— even if they were not entirely consistently estimated in Ref. [10] constitute a small correction. It is important to
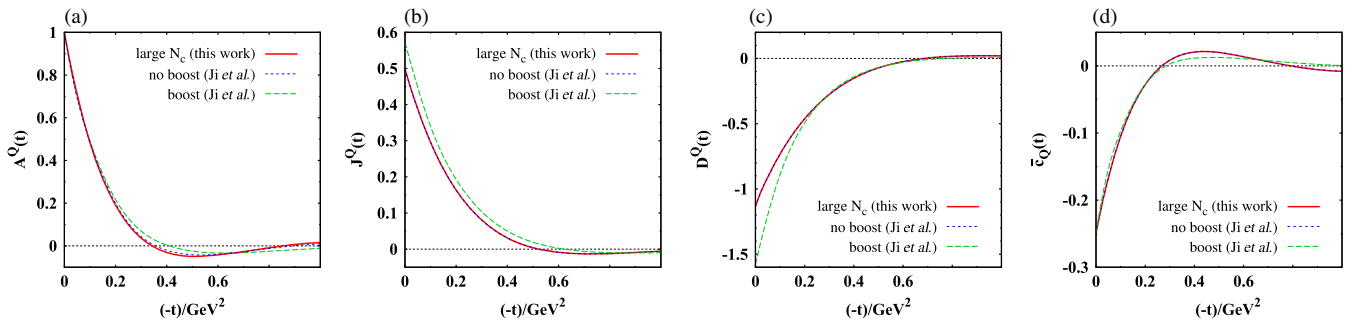

FIG. 1. EMT form factors of quarks in the bag model in the large-N_c limit (solid lines, this work). For comparison, we also show results by Ji *et al.*, Ref. [10], computed in the bag model without (dotted lines) and with (dashed lines) considering boosts. This comparison shows the effects of relativistic and $1/N_c$-corrections within the "independent-particle model treatment" in the bag model. For finite N_c, there are further corrections associated with the independent-particle model treatment; see the text.

stress that in the large-N_c limit $|\vec{\Delta}|/(2M_N) \to 0$ and this type of relativistic corrections is negligible.

The third type of $1/N_c$ corrections is due to the fact that the bag model belongs to a class of so-called independent-particle models in which the form factors of one-body operators are strictly speaking zero; the transferred momentum is absorbed by only one "active quark," while the motion of the remaining "spectator" quarks is not affected. The nucleon wave function of such a configuration is strictly speaking zero. In a more realistic description, the nucleon wave function would contain "correlations" between the constituents through which the momentum transferred to the active quark would be redistributed among all constituents of the system such that the nucleon as a whole would recoil [10]. But the bag model quark wave functions are independent of each other, and lack explicit correlations.

At least in principle, the bag model could provide correlations: the elastic scattering process could be thought of as consisting of two steps. In the first step, the active quark absorbs the transferred momentum. In the second step, the active quark "bounces off" the bag boundary, which subsequently transfers momentum to the spectator quarks, etc. Through such back-and-forth bouncing, the transferred momentum would be redistributed among all constituents. For larger $|t|$, inelastic processes (bag deformation and the creation of $\bar{q}q$-pairs) may become possible. Even though this simple mechanism cannot be expected to be realistic, at least in principle, one could estimate correlation effects in this way. In practice, this is too complex to consider, and a different way to heuristically estimate correlation effects was chosen in Ref. [10]: a free parameter η was introduced such that the momentum transfer to the active quark is $\vec{\Delta} \to \eta\vec{\Delta}/\cosh(w)$. It is intuitively expected that $\eta \sim 1/3$ to redistribute the momentum transfer among three quarks in a recoiled nucleon. A reasonable description of the proton electromagnetic form factors was obtained for η in the range of $\eta = 0.35$–0.55 with the lower (higher) value yielding a better description of the data at large (intermediate) values of $|t|$ [10]. The correlations modeled in this way impact the EMT form factors more strongly than the two above-discussed types of $1/N_c$ corrections. However, the discrepancy with the general constraints at $t = 0$ becomes also more pronounced: e.g., for $\eta = 0.35$, one finds $J^Q(0) \approx 0.25$ [10] instead of $J^Q(0) = \frac{1}{2}$, indicating that this method to estimate correlation effects is not trustworthy at small $|t|$, even though it improves the phenomenological description of electromagnetic form factors at $|t| \lesssim 2$ GeV^2 [10]. As our large-N_c results are valid for small $|t| \ll M_N^2$, while the results for $\eta \neq 1$ from Ref. [10] are more appropriate at larger $|t|$, a direct comparison is not meaningful, and we refrain from it.

Notice that in the large-N_c limit also this type of corrections vanishes. Let us recall that correlations were introduced to allow the active quark to redistribute the

momentum transfer among all constituents such that the entire system changes its direction and the nucleon as a whole is deflected. However, in the leading order of the large-N_c limit, the momentum transfer is small, $|t| \ll M_N^2$, and the recoil of the heavy nucleon ($M_N \sim N_c$) is negligible. Thus, one can consistently evaluate form factors in the bag model without the need to introduce correlations. (Notice that the absence of correlations in the large-N_c limit is a peculiarity of the bag model. Other models formulated in the large-N_c limit like the chiral quark soliton or Skyrme models [16–23] exhibit strong correlations.)

To summarize, we may regard the results for the EMT form factors shown in Fig. 1 as valid for $|t| \ll M_N^2$ and theoretically consistent within the bag model in the large-N_c limit. These results are subject to $1/N_c$ corrections which we may expect to be modest at smaller $|t|$ and more sizable especially at larger $|t|$. Our observations are in line with results from the Skyrme model of Ref. [88] where relativistic recoil corrections (to electromagnetic form factors) were also found small for $|t| < 1$ GeV^2.

V. EMT DENSITIES IN BAG MODEL

In order to compute the EMT densities, one can perform the Fourier transforms in Eq. (3). In the large-N_c limit in the bag model, one can also directly evaluate the EMT matrix elements in coordinate space. Both ways yield the same result for quark EMT densities. But only the direct evaluation in coordinate space allows us to compute the contributions of the gluons in $\mathcal{L}_G$ and the "quark-gluon interaction" in $\mathcal{L}_{\text{surf}}$ as defined in (8). We obtain

$$T_q^{00}(r) = \frac{N_q A^2}{4\pi}\frac{\Omega}{R}(\alpha_+^2 j_0^2 + \alpha_-^2 j_1^2)\Theta_V, \tag{24a}$$

$$T_q^{0k}(\vec{r}) = -\frac{1}{2}\frac{P_q A^2}{4\pi}\left(2\alpha_+\alpha_-\frac{\Omega}{R}j_0 j_1 + \alpha_-^2\frac{j_1^2}{r}\right)\epsilon^{klm}e_r^l S^m\Theta_V, \tag{24b}$$

$$T_q^{ik}(\vec{r}) = \frac{N_q A^2}{4\pi}\alpha_+\alpha_-\left(\left(j_0 j_1' - j_0' j_1 - \frac{j_0 j_1}{r}\right)e_r^i e_r^k\right.$$
$$\left. + \frac{j_0 j_1}{r}\delta^{ik}\right)\Theta_V, \tag{24c}$$

$$T_G^{\mu\nu}(r) = g^{\mu\nu}B\Theta_V, \tag{24d}$$

$$T_{\text{surf}}^{\mu\nu}(\vec{r}) = 0. \tag{24e}$$

For brevity, we suppress the arguments of the Bessel functions $j_i = j_i(\omega r/R)$, and primes denote differentiation with respect to r. The quark flavor dependence is encoded in the SU(4) spin-flavor factors (17). The contribution of $\mathcal{L}_{\text{surf}}$ vanishes, but we obtain the contribution $T_G^{\mu\nu}(r) = g^{\mu\nu}B\Theta_V$ associated with nonfermionic (gluonic) effects.

A. Energy density and mass

The energy density $T_{00}(r)$ receives the contribution $T_{00}^Q(r)$ from quarks, Eq. (24a), and a contribution from gluons $T_{00}^G(r) = B\Theta_V$ in Eq. (24d). The quark and gluon contributions to the energy density are shown in Fig. 2(a). The integrated contributions are

$$M_N^Q = N_c\varepsilon_0, \qquad M_N^G = \frac{4\pi}{3}R^3 B. \qquad (25)$$

For massless quarks, the relative contributions of quarks and gluons to the nucleon mass are $M_N^Q : M_N^G = 3:1$. This can be derived in two ways: (i) it follows from the nonlinear bag boundary condition (10c), and, equivalently, (ii) it can be derived from minimizing the nucleon mass understood as a function of R as follows. Since $\varepsilon_0 = \omega_0/R$, we have

$$M_N'(R) = \frac{\partial}{\partial R}\left(N_c\frac{\omega_0}{R} + \frac{4\pi}{3}R^3 B\right) \stackrel{!}{=} 0 \Leftrightarrow N_c\omega_0 = 4\pi R^4 B. \qquad (26)$$

From Eqs. (25) and (26), we see that $M_N^Q = \frac{3}{4}M_N$ and $M_N^G = \frac{1}{4}M_N$ (for massless quarks). This can be viewed as a bag-model version of the "virial theorem." We recall that e.g., in soliton models virial theorems are derived by rescaling the coordinates $\vec{r} \to \lambda\vec{r}$ in the functional defining the nucleon mass. Considering infinitesimal variations around $\lambda = 1$ leaves the nucleon mass invariant, i.e., $\delta M_N = 0$. This implies relations among different contributions to the nucleon mass [16,19]. In the bag model, the situation is simpler: the "variation" of the nucleon mass assumes the simple form stated in Eq. (26) for massless quarks. For massive quarks, $\omega_0 = \omega_0(mR)$ depends also on R, and the virial theorem has a somewhat different form; see Appendix A 1. Notice that (26) shows that the constant $B = \mathcal{O}(N_c)$ where one has to keep in mind that the bag radius $R = \mathcal{O}(N_c^0)$ since the size of baryons is of order N_c^0 in the large-N_c limit.

B. Angular momentum density

The components $T_{0k}(\vec{r})$ depend on the nucleon polarization (which we do not indicate for brevity), and receive only a contribution from quarks. The angular momentum density is given by

$$J_q^i(\vec{r}) = \epsilon^{ijk}r^j T_q^{0k}(\vec{r})$$
$$= S^m\left[\delta^{im}\rho_J^q(r)_{\text{mono}} + \left(e_r^i e_r^m - \frac{1}{3}\delta^{im}\right)\rho_J^q(r)_{\text{quad}}\right], \qquad (27)$$

with the monopole [16] and quadrupole [70] contributions

$$\rho_J^q(r)_{\text{mono}} = -\frac{2}{3}\rho_J^q(r)_{\text{quad}} \equiv \rho_J^q(r),$$
$$\rho_J^q(r) = \frac{1}{3}\frac{P_q A^2}{4\pi}r\left(\frac{2\Omega}{R}\alpha_+\alpha_- j_0 j_1 + \alpha_-^2 \frac{j_1^2}{r}\right)\Theta_V. \qquad (28)$$

The relation $\rho_J^q(r)_{\text{mono}} = -\frac{2}{3}\rho_J^q(r)_{\text{quad}}$ is a general result [71] which the bag model respects. The total angular momentum density $\rho_J(r) = \sum_q \rho_J^q(r)$ is normalized as $\int d^3r\,\rho_J(r) = \frac{1}{2}$ and shown in Fig. 2(b).

C. Shear forces and pressure

The pressure and shear forces encoded in the stress tensor (5) are given by the expressions

$$p(r) = \left[\frac{N_c A^2}{12\pi}\alpha_+\alpha_-\left(j_0 j_1' - j_0' j_1 + \frac{2}{r}j_0 j_1\right) - B\right]\Theta_V,$$
$$s(r) = \left[\frac{N_c A^2}{4\pi}\alpha_+\alpha_-\left(j_0 j_1' - j_0' j_1 - \frac{1}{r}j_0 j_1\right)\right]\Theta_V. \qquad (29)$$

The numerical results for massless quarks are shown in Figs. 2(c) and 2(d).

In the liquid drop model of a large nucleus which exhibits a "sharp edge" at the radius R_{nucl}, the shear force
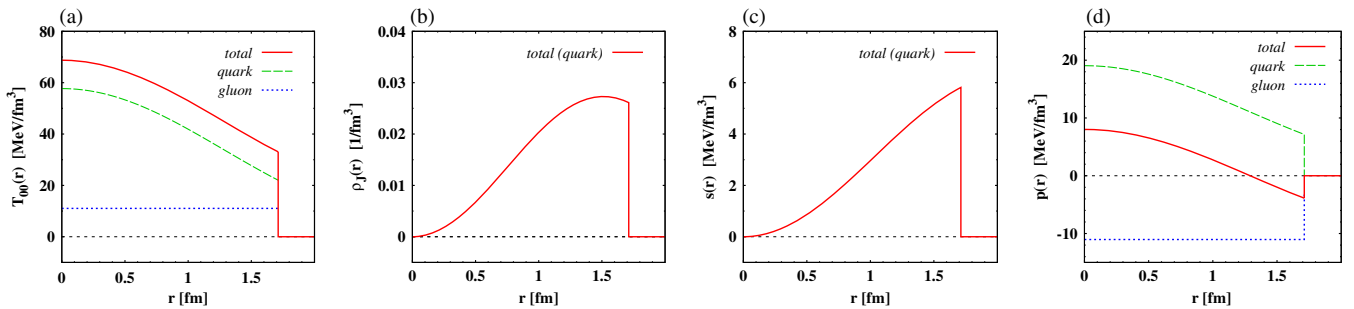

FIG. 2. (a) The energy density $T_{00}(r)$, (b) density $\rho_J(r)$ characterizing the angular momentum density, (c) shear force distribution $s(r)$, and (d) pressure distribution $p(r)$ as functions of r in the bag model for massless quarks. The vertical lines mark the position of the bag boundary (at $R = 1.71$ fm for massless quarks). In the case of $T_{00}(r)$ and $p(r)$, the contributions from quarks and gluons are shown in addition to the total result. For $\rho_J(r)$ and $s(r)$, the total result is entirely due to quarks.

is given by $s(r) = \gamma \delta(r - R_{\text{nucl}})$ where γ is the surface tension [8]. The nucleon is a far more diffuse object than a large nucleus, and Fig. 2(c) shows that $s(r)$ is consequently much more "spread out" than a δ-function characterizing the shear force distribution of a large nucleus.

In all model calculations so far, the pressure was found positive in the inner region and negative in the outer region. This is also the case in the bag model; see Fig. 2(d). The positive pressure in the inner region is associated with repulsive forces directed toward the outside. The negative pressure in the outer region corresponds to attractive forces directed toward the inside. The repulsive and attractive forces must compensate each other according to the von Laue condition, which is a necessary condition for stability and will be discussed below in Sec. V F.

The pressure distribution and the shear forces in Eq. (29) satisfy the differential equation (6). This relation is a consequence of the conservation of the EMT, $\partial_\mu T^{\mu\nu} = 0$, and hence reflects the fact that in the bag model the EMT is conserved and the description is internally consistent.

D. Normal and tangential forces

The stress tensor (5) is a symmetric 3×3 matrix of which the eigenvectors are the unit vectors $\vec{e}_r$, $\vec{e}_\vartheta$, $\vec{e}_\varphi$ of the spherical coordinate system and eigenvalues are related to normal and tangential forces [9]. For spin-0 and spin-$\frac{1}{2}$ particles, the tangential eigenvalues (pertaining to eigenvectors $\vec{e}_\vartheta$, $\vec{e}_\varphi$) are degenerate with the degeneracy being lifted only for higher spin $J \geq 1$ particles. In our case, the normal and tangential forces per unit area are given by [9]

$$T^{ij} dA_r^j = \frac{dF_n}{dA_r} dA_r e_r^i = \left(\frac{2}{3} s(r) + p(r) \right) dA_r e_r^i,$$

$$T^{ij} dA_\vartheta^j = \frac{dF_t}{dA_\vartheta} dA_\vartheta e_\vartheta^i = \left(-\frac{1}{3} s(r) + p(r) \right) dA_\vartheta e_\vartheta^i, \quad (30)$$

where $d\vec{A}_r = dA_r \vec{e}_r$, etc., denote the corresponding infinitesimal area elements. The results for normal forces dF_n/dA_r and tangential forces $dF_t/dA_\vartheta = dF_t/dA_\varphi$ are shown in Fig. 3.

Mechanical stability requires that $dF_n/dA_r \geq 0$ with strictly $dF_n/dA_r > 0$ at all values of r within the system [23]. The position where $dF_n/dA_r = 0$ marks the "end" of the system [9]. In the bag model, it is consequently $dF_n/dA_r > 0$ for $0 \leq r < R$, and the normal force vanishes at the finite radius $r = R$, as shown in Fig. 3(a). This is a distinctly different situation than in soliton models where $dF_n/dA_r > 0$ for all $0 \leq r < \infty$ and the normal forces vanish only in the limit $r \to \infty$ [16–23]. Other examples of finite size systems which are analogous in the sense that dF_n/dA_r vanishes at a finite radius are the liquid drop model [8] and neutron stars of which the radius is defined
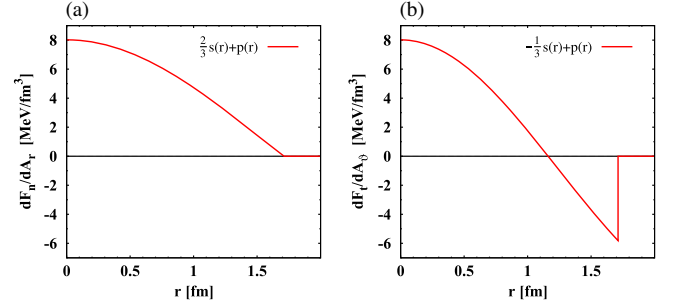

FIG. 3. Densities of (a) normal $dF_n/dA_r = \frac{2}{3} s(r) + p(r)$ and (b) tangential $dF_t/dA_\vartheta = dF_t/dA_\varphi = -\frac{1}{3} s(r) + p(r)$ forces per unit area in the bag model as functions of r. Mechanical stability requires $\frac{2}{3} s(r) + p(r) > 0$ inside the bag, which is the case.

as that value of r where the normal force per unit area (also called the hydrostatic pressure) vanishes [89].

E. Mechanical radius, surface tension, and diffusiveness

The positivity of the normal forces allows one to introduce the notion of a mechanical radius defined as [9]

$$\langle r^2 \rangle_{\text{mech}} = \frac{\int d^3 r \, r^2 [\frac{2}{3} s(r) + p(r)]}{\int d^3 r [\frac{2}{3} s(r) + p(r)]}. \quad (31)$$

We obtain $\langle r^2 \rangle_{\text{mech}}^{1/2} = 1.10$ fm, which is smaller than the proton charge radius $\langle r^2 \rangle_{\text{el}}^{1/2} = 1.25$ fm with our parameters. The values of the radii depend on how model parameters are fixed; e.g., a smaller proton charge radius of 1 fm was found in Ref. [60] with a different parameter fixing. A more robust prediction might be the ratio $\langle r^2 \rangle_{\text{mech}}^{1/2} / \langle r^2 \rangle_{\text{el}}^{1/2} = 0.88$ which is independent of how model parameters are fixed (for massless quarks). Interestingly, also the chiral quark soliton model predicts the mechanical radius to be smaller than the proton charge radius (by 25% in that model) [9]. Notice that the mechanical radius is the same for the proton and neutron modulo small isospin violating effects, and hence constitutes a better concept for the nucleon "size" than the charge radius (which is negative for the neutron, giving insights on the distribution of charge inside neutron but not on its size).

One may define the property of "surface tension" for a hadron as

$$\gamma = \int_0^\infty dr \, s(r), \quad (32)$$

if this integral exists. In the bag model, we find $\gamma = 4.26$ MeV/fm^2. The concept of a surface tension is well justified in certain situations, for instance for large nuclei [8] or Q-balls [34]. The nucleon is much more diffuse. In order to quantify the "diffusiveness" of a particle, we

introduce the dimensionless measure Δw^2 for the "skin thickness" of a particle defined in terms of the moments $\langle r^n \rangle_s$ of the shear force distribution as follows [34]:

$$\Delta w^2 = \frac{\langle [r^2 - \langle r^2 \rangle_s]^2 \rangle_s^{1/2}}{\langle r^2 \rangle_s} = \frac{[\langle r^4 \rangle_s - \langle r^2 \rangle_s^2]^{1/2}}{\langle r^2 \rangle_s},$$

$$\langle r^n \rangle_s = \frac{1}{\gamma} \int dr \, r^n s(r). \qquad (33)$$

For a nucleus with a sharp edge in the liquid drop model, the shear force is given by $s(r) = \gamma \delta(r - R_A)$ where R_A denotes the radius of the nucleus, and $\Delta w^2 = 0$. One also finds $\Delta w^2 \to 0$ in the limit of very large Q-balls [34]. For realistic nuclei and finite-size Q-balls, the diffusiveness parameter Δw^2 is small. For the nucleon, $\Delta w^2 = 0.48$ in the bag model, indicating that the nucleon is much more diffuse than a nucleus, which is not unexpected.

F. EMT conservation: Von Laue condition and its lower-dimensional analogs

The pressure and shear forces must obey the following integral relations:

$$\int_0^\infty dr \, r^2 p(r) = 0,$$

$$\int_0^\infty dr \, r \left(-\frac{1}{3} s(r) + p(r) \right) = 0,$$

$$\int_0^\infty dr \left(-\frac{4}{3} s(r) + p(r) \right) = 0. \qquad (34)$$

The first of these relations was introduced by von Laue in Ref. [90] and holds in three dimensions; the other two hold in respectively two dimensions and one dimension and were derived in Ref. [9].

The conditions in (34) are proven analytically in Appendix A 2. The physical interpretation of the first

condition in (34) is as follows. The positive pressure in the inner region corresponds to repulsion, and the negative pressure in the outer region corresponds to attraction. Mechanical stability requires that the attractive and repulsive forces compensate each other in the 3D integral in (34) which is satisfied in the bag model as shown in Fig. 4(a). The tangential force per unit area, $-\frac{1}{3} s(r) + p(r)$, must satisfy the two-dimensional (2D) relation in (34), which is the case in the bag model as illustrated in Fig. 4(b). The interpretation of this condition is that the tangential forces within a 2D slice must compensate each other [9]. Similarly, also the one-dimensional (1D) condition in (34) is satisfied in the bag model, which is illustrated in Fig. 4(c). It is also instructive to discuss the "finite-volume von Laue condition" [9]

$$\int_{|\vec{r}'| \le r} d^3 r' \, p(r') = V(r) \left(\frac{2}{3} s(r) + p(r) \right), \qquad (35)$$

where the integration goes over the volume $V(r) = \frac{4}{3} \pi r^3$. The sum rule (35) is satisfied for all $0 \le r < R$. However, in the bag model at $r = R$, one practically deals with the 3D relation in (34). Since $V(R) \ne 0$ is nonzero, this means that the normal force per unit area $\frac{2}{3} s(r) + p(r)$ must vanish at the bag boundary, which is the case and emerges here as a necessary condition to comply with the von Laue condition in (34). Notice that $\frac{2}{3} s(r) + p(r)$ must vanish at the bag boundary also in order to comply with (6). The differentiation of Θ_V-functions in the bag model expressions (29) for $p(r)$, $s(r)$ yields the contribution $\delta(r - R)[\frac{2}{3} s(r) + p(r)]$ to (6), which must and does vanish at $r = R$.

The integrands $p^{(3D)}(r) = p(r)$, $p^{(2D)}(r) = -\frac{1}{3} s(r) + p(r)$, and $p^{(1D)}(r) = -\frac{4}{3} s(r) + p(r)$ in (34) are special cases of pressures in n-dimensional (nD) spherically symmetric mechanical systems. In general, the pressure and shear forces of a kD system are related to those in nD
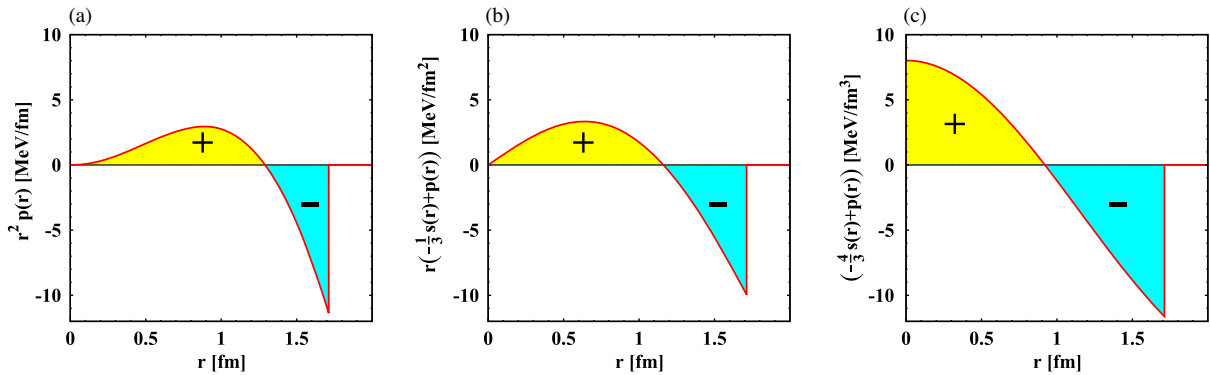

FIG. 4. The 3D von Laue condition (a) and its lower-dimensional analogs in two dimensions (b) and one dimension (c) in the bag model for massless quarks. The areas above and below the *r*-axis are equal and compensate each other according to the integrals in Eq. (34).

subsystems (if $k < n$, the roles of system and subsystem interchange) as [91]

$$p^{(nD)}(r) = \frac{k}{n}p^{(kD)}(r) + \frac{k(n-k)}{n}\frac{1}{r^k}\int_0^r dr'\,r'^{k-1}p^{(kD)}(r'),$$

$$s^{(nD)}(r) = -\frac{k}{n-1}p^{(kD)}(r) + \frac{k^2}{n-1}\frac{1}{r^k}\int_0^r dr'\,r'^{k-1}p^{(kD)}(r').$$
(36)

The $s^{(nD)}(r)$ and $p^{(nD)}(r)$ in (36) satisfy $\frac{n-1}{n}\frac{\partial}{\partial r}s^{(nD)}(r) + \frac{n-1}{r}s^{(nD)}(r) + \frac{\partial}{\partial r}p^{(nD)}(r) = 0$ and $\int_0^\infty dr\,r^{n-1}p^{(nD)}(r) = 0$, which are nD-versions of respectively (6) and (34). Such relations can be useful e.g., in holographic approaches to QCD or in fractal theories [91]. In the bag model, these relations are valid for all $n, k > 0$ including noninteger and arbitrarily large values. The practical verification of such relations can in practice be numerically challenging especially for large n. In the bag model, thanks to the finite range of the densities, it is possible to test the validity and consistency of the relations (36) for any value of $n, k > 0$ in a nontrivial model.

G. EMT conservation: Equivalence of *D*-term expressions

The *D*-term can be computed using the expressions in terms of (i) pressure and (ii) shear forces according to Eq. (7). From (29), we find that the two equivalent expressions in Eq. (7) yield the same result, which can be written as

$$D = \frac{1}{3}M_N N_c \frac{A^2 R^4}{\omega_0^4}\alpha_+\alpha_-\left(-\frac{4}{15}\omega_0^3 + \omega_0 \right.$$
$$\left. - \frac{2}{5}\omega_0\sin^2\omega_0 - \sin\omega_0\cos\omega_0\right);$$
(37)

see Appendix A 3 for a detailed proof. The possibility to compute the *D*-term by means of two different equivalent expressions is also due to EMT conservation. We will discuss the *D*-term in Sec. VI in more detail.

H. EMT conservation: Form factor $\bar{c}^G(t)$

In Sec. IV, we found the form factor $\bar{c}^Q(t) \neq 0$ from the evaluation of the quark EMT, which means that $T^Q_{\mu\nu}$ by itself is not conserved. EMT conservation requires $\sum_a \bar{c}^a(t) = 0$ if one takes into account all contributions in a system, i.e., in the bag model also the contribution of the bag which simulates gluons in the sense discussed in Sec. III. However, while it was straightforward to compute

the quark EMT form factors in Sec. IV, it is not clear how to compute the bag contribution to the form factors. At this point, we can take advantage of the EMT density framework. Instead of using EMT form factors as an input for an interpretation in terms of EMT densities [8], we proceed in the opposite direction and invert Eq. (3) for the gluon contribution $T^G_{\mu\nu}(r)$ in Eq. (24d). We obtain for massless quarks the result

$$\bar{c}^G(t) = \frac{1}{M_N}\int d^3r\exp(i\vec{\Delta}\vec{r})B\Theta_V = \frac{3}{4}\frac{j_1(qR)}{qR}, \quad q = \sqrt{-t},$$
(38)

where we eliminated the bag constant B by means of Eq. (26). From the behavior of spherical Bessel functions for small arguments $j_l(z) = z^l/(2l + 1)!! + \mathcal{O}(z^{l+2})$, we find $\bar{c}^G(0) = \frac{1}{4}$ to be compared with $\bar{c}^Q(0) = -\frac{1}{4}$; see Sec. IV C and Fig. 1(d). In Appendix, we show that we have $\forall\, t$,

$$\bar{c}^Q(t) + \bar{c}^G(t) = 0,$$
(39)

as it is required by the conservation of the total EMT.

VI. *D*-TERM

In this section, we discuss the *D*-term for the nucleon and other hadrons, and we consider then several instructive limiting cases in the bag model. Here and throughout in Secs. VI A–VI F, we consider massless quarks. In Sec. VII, we will discuss also $m \neq 0$. The expression for the *D*-term of the nucleon was already quoted in (37). Let us generalize this result to a general state. Mesons (baryons) are constructed in the bag model by placing a $\bar{q}q$ (qqq) in the bag in a color singlet state. The mass and bag radius of a general bag model state (for massless quarks) are given by

$$M = \frac{4}{3}\frac{\sum_i \omega_i}{R}, \qquad R = \left(\frac{\sum_i \omega_i}{4\pi B}\right)^{1/4},$$
(40)

which follows from the virial theorem (26). For baryons, the summation goes over $N_c = 3$ occupied bag levels ω_i, for mesons over two levels. The bag constant is fixed as $B = 0.0559$ fm^{-4} to reproduce the nucleon mass. Inserting the expressions for the normalization constant A and $\alpha_\pm$ defined in (11) and mass (40) into Eq. (37), we obtain the result for the *D*-term of a general bag model state (made of massless quarks)

$$D = -\frac{4}{5}\times\left[\sum_{i=1}^{N_{\text{cons}}}\omega_i\right]\left[\sum_{i=1}^{N_{\text{cons}}}\frac{\omega_i(4\omega_i^2 - 15) + 6\omega_i\sin^2\omega_i + 15\sin\omega_i\cos\omega_i}{54\omega_i(\omega_i - 1)\sin^2\omega_i}\right].$$
(41)

We make two important observations. First, since $\omega_i \geq \omega_0 \approx 2.04$, it is $D < 0$ for all hadron states constructed in the bag model including unstable resonances. This is in line with results from all theoretical studies so far. Second, the dependence on the model parameter bag radius R or bag constant B cancels out in the D-term, which therefore only depends on the dimensionless numbers ω_i (for massless quarks, cf. Sec. VII for the case of massive quarks).

A. D-term of the nucleon

For the nucleon, we obtain from (37) and (41) in the case of massless quarks the result

$$D_{\text{nucleon}} = -1.145, \qquad (42)$$

which is in agreement with the numerical bag model calculation of nucleon GPDs and EMT form factors in Ref. [10]. The magnitude of the nucleon D-term in the bag model is smaller compared to soliton models [16–23]. This is not surprising considering that $D = M_N \int d^3 r\, r^2 p(r)$ is sensitive to long distances. In fact, in chiral models, $|D|$ is larger in the chiral limit where $p(r)$ and $s(r) \propto 1/r^6$. For finite pion masses m_π, the densities decay exponentially like $e^{-m_\pi r}$. The range of internal forces decreases in the soliton models, and $|D|$ diminishes [16]. Since the bag model has a finite radius, the value for $|D|$ is small. We remark that through the SU(4) spin-flavor factors (17) the bag model complies with the large-N_c predictions [6]

$$(D^u + D^d)_{\text{nucleon}} = \mathcal{O}(N_c^2), \quad (D^u - D^d)_{\text{nucleon}} = \mathcal{O}(N_c).$$
$$(43)$$

B. ρ-meson

Placing in the lowest level of the bag a $\bar{q}q$ pair with aligned spins yields a state with the quantum numbers of a ρ-meson. When B is fixed to reproduce the nucleon mass, one obtains a ρ-meson mass of 692 MeV. This is within 10% of the experimental ρ-meson mass value of 775 MeV. Other ways to fix model parameters can also be considered [92]. In contrast to this, there is no ambiguity as to the bag model prediction for the D-term (41) which does not depend on the bag radius R or bag constant B. The model prediction is

$$D_{\rho\text{-meson}} = \frac{4}{N_c^2} D_{\text{nucleon}} = -0.509. \qquad (44)$$

Recalling that $D_{\text{nucleon}} = \mathcal{O}(N_c^2)$, cf. (43), we see that the D-term of the ρ-meson (and all mesons) is of $\mathcal{O}(N_c^0)$.

As there is no spin-spin interaction, a $\bar{q}q$ pair with antialigned spins corresponding to a state with pion quantum numbers has exactly the same mass (and D-term) as the ρ-meson. However, since the bag boundary does not respect chiral symmetry, the description of the pion in the bag model is inadequate. This becomes evident here in two

ways. First, in the chiral limit, the pion is massless, while here it remains massive and is mass degenerate with the ρ-meson. Second, soft pion theorems predict $D_{\text{pion}} = -1$ [93–96], while in the bag model, one would obtain the same value as in (44). Ways to construct light pion states have been discussed [97]. The cloudy bag model [98] reconciles the bag concept and chiral symmetry. Both approaches are beyond the scope of this work. In any case, since it is not a Goldstone boson, one may apply the bag model to the description of the ρ-meson with fewer reservations. It will be interesting to test the bag model prediction $D_{\rho\text{-meson}} : D_{\text{nucleon}} = 4:9$ in other models or lattice QCD.

Notice that a spin-1 hadron like the ρ-meson has six form factors of the total EMT [24,76,77]. Our $D_{\rho\text{-meson}}$ corresponds to the form factor $D_0(t)$ in the notation of Ref. [76] and to $-\mathcal{G}_3(t)$ in [77]. Studies of other ρ-meson EMT form factors will be left to future investigations.

C. Δ-resonance

Let us briefly also comment on the D-term of the Δ-resonance. As discussed in the previous section, due to the absence of spin-spin interactions, states differing by the spin quantum numbers are degenerate. In particular, also the Δ-resonance and the nucleon are degenerate, and the D-term of the Δ is simply predicted to be

$$D_{\Delta\text{-resonance}} = D_{\text{nucleon}} = -1.145. \qquad (45)$$

Even though the absolute value might be underestimated, the bag model result $D_{\Delta\text{-resonance}} = D_{\text{nucleon}}$ is correct in large N_c [23]. This is another consistency test of the large-N_c description of baryons in the bag model.

D. Roper resonance

The state $N(1440)$ known as Roper resonance has the quantum numbers of the proton $J^P = \frac{1}{2}^+$, but a 50% larger mass and its structure "has defied understanding" since its discovery in the 1960s; see the review in Ref. [99]. In the bag model, it is described by placing two quarks in the ground state with $\omega_0 = 2.04$ and one quark in the first excited state with $\omega_1 = 5.40$. If one would use the same bag radius for the nucleon and the Roper, then the physical value of the Roper mass would be reproduced. A more consistent parameter treatment may be to use the same bag constant B for the nucleon and Roper, which yields a Roper mass of 1302 MeV and underestimates the physical value by 10%. This is not unreasonable for such a simple model. While the mass increases by about 50%, the pressure in the center increases by a factor of 7.5 as one goes from the ground state nucleon to the first excited state in the $J^P = \frac{1}{2}^+$ sector. The increase of the internal forces is reflected by an increase of the D-term for which Eq. (41) yields the value

$$D_{\text{Roper}} = 5.846\, D_{\text{nucleon}} = -6.695. \qquad (46)$$

It is interesting to observe how strongly the D-term is varied as one goes from a ground state to an excited state within a theory. This is mainly due to an increase of internal forces, and in line with studies of excited states in Q-ball systems [35]. It is not known how the D-term of the Roper can be studied in experiment, but it would be interesting to confront the prediction (46) with results from other models or lattice QCD. We remark that Δw^2 defined in (33) is for Roper $\Delta w^2 = 0.72$ showing that this state is even more diffuse than the nucleon, as intuitively expected.

E. Negative parity baryons

The lightest baryon with quantum numbers $J^P = \frac{1}{2}^-$ is $N(1535)$. Negative parity solutions to the bag equations (10) are given by the same expression as positive parity solutions (11), but with upper and lower components exchanged and with the ω_i obtained from (for massless quarks) the transcendental equation $\omega = (1 + \omega) \tan \omega$ of which the lowest energy solution is $\omega = 3.81$. Keeping B fixed at the value required for the nucleon yields 1498 MeV and reproduces the mass of $N(1535)$ within 3%. Also, here is the D-term independent of parameter fixing, and we obtain

$$D_{N(1535)} = 11.32\, D_{\text{nucleon}} = -12.97, \qquad (47)$$

which confirms the trend that the D-terms grow for heavier excited states in the spectrum of a theory. Also in this case, we are not aware of a practical method to learn about the D-term of the state $N(1535)$ from experiment. However, the interesting prediction $D_{N(1535)} = 11.32 D_{\text{nucleon}}$ could be compared to theoretical studies in other models. With $\Delta w^2 = 0.59$, this state is somewhat less diffuse than the Roper.

F. Highly excited states in baryonic spectrum

In this section, we consider higher excited states in the bag model. While we do not expect a realistic description of the hadronic spectrum, the bag model provides a consistent theoretical framework, and it is instructive to explore it. For simplicity, we consider massless quarks and limit ourselves to the positive parity baryons sector.

As mentioned in the context of Eq. (41), we find $D < 0$ for all excited states. Another important observation is that the D-terms grow quickly with the mass of the hadron. To illustrate this point, we plot the D-terms vs masses for $J^P = \frac{1}{2}^+$ baryons made of massless u- and d-quarks in Fig. 5, which shows the first 4000 states: the first state is the nucleon with $(M, D) = (938 \text{ MeV}, -1.145)$, and the last state has $(M, D) = (10.9 \text{ GeV}, -3068)$. All states above 2 GeV are hypothetical and practically in the continuum. Each state has a twofold degeneracy due to isospin quantum numbers. (In our large-N_c treatment, the spectrum of $J^P = \frac{3}{2}^+$ baryons looks exactly the same with a fourfold degeneracy due to isospin $\frac{3}{2}$ of Δ-states.) While the baryon
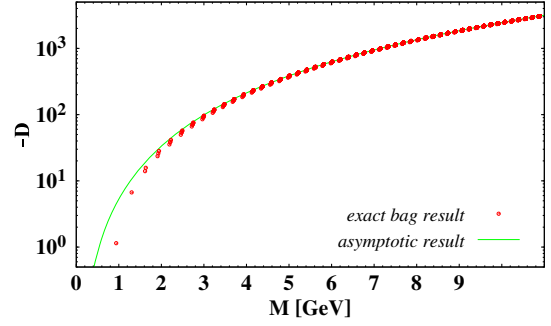

FIG. 5. $(-D)$ vs mass for the first 4000 states in the positive parity sector for states made of massless up- and down-quarks. While the masses increase by 1 order of magnitude, the D-terms grow by 4 orders of magnitude. The analytically derived asymptotic result (50) for the D-term is shown as solid line. The degeneracy pattern of the states is explained in the text.

masses increase by 1 order of magnitude in the range considered in Fig. 5, the D-terms grow by 4 orders of magnitude. This is in line with results from Q-balls [35].

To get more insight, we discuss the EMT densities of a (hypothetical) highly excited nucleon state. For Q-balls, it was observed that $T_{00}(r)$ of the Nth (radial) excitation exhibits characteristic structures with N-shells surrounding a "core" region, while $p(r)$ exhibits $(2N + 1)$-nodes where $N = 0$ refers to the ground state [35]. Is this also the case for excited states in the bag? The answer is no. For illustration, we show in Fig. 6 the EMT densities for the state with the level ω_{15} triply occupied. This corresponds to a hypothetical 3163th excited state above the nucleon (ground) state with $(M, D) = (10.2 \text{ GeV}, -2608)$. The EMT densities exhibit characteristic "wiggles," but $p(r)$ exhibits only one node. This is a general result; no matter how highly excited a bag state is, $p(r)$ crosses zero only once. Clearly, the spectrum of excitations in the bag model has a much different structure than the Q-ball system [35]. One expects such highly excited states to be very diffuse, and the result $\Delta w^2 = 2.9$ for this hypothetical state confirms it.

The solutions to the transcendental equation (12) are approximated by $\omega_j \to (j + 3/4)\pi$ for massless quarks to within an accuracy of better than 2% already for $j \geq 1$. For ω_{15}, this asymptotic formula has an accuracy of 2×10^{-4}. Evaluating the expressions for $T_{00}(r)$, $p(r)$, and $s(r)$ in Eqs. (24a), (24d) and (29) for asymptotically large ω_j yields

$$[r^2 T_{00}(r)]_{\text{asymp}} = \frac{\sum_j \omega_j}{4\pi R^2}\left(1 + \frac{r^2}{R^2}\right)\Theta_V,$$

$$[r^2 p(r)]_{\text{asymp}} = \frac{\sum_j \omega_j}{4\pi R^2}\left(\frac{1}{3} - \frac{r^2}{R^2}\right)\Theta_V,$$

$$[r^2 s(r)]_{\text{asymp}} = \frac{\sum_j \omega_j}{4\pi R^2}\Theta_V \quad \text{for } \omega_j \to (j + 3/4)\pi, \quad (48)$$
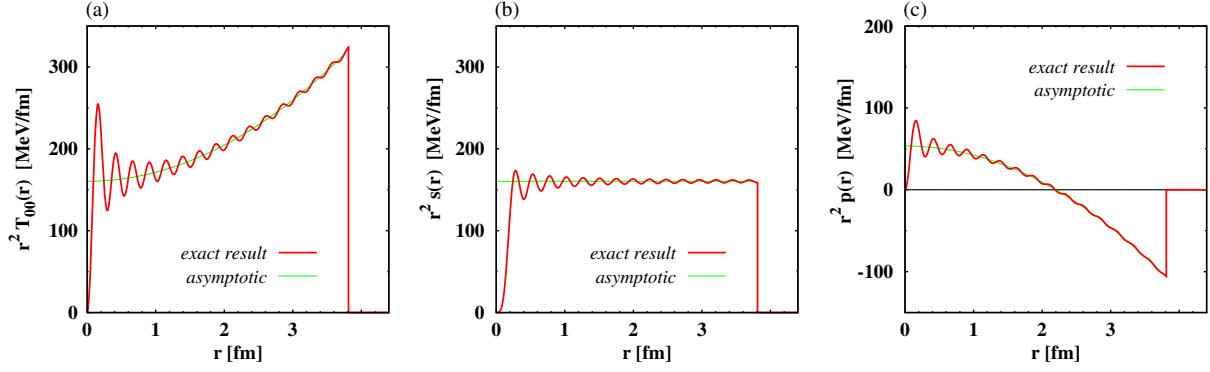
FIG. 6.   Solid lines: EMT densities $r^2 T_{00}(r)$, $r^2 s(r)$, and $r^2 p(r)$ for a (hypothetical) highly excited nucleon state with the triply occupied bag level $\omega_{15} = 49.47 \approx (j + 3/4)\pi$ with $j = 15$. For this state, the bag radius is $R = 3.8$ fm, mass $M = 10.24$ GeV, and D-term $D = -2607.7$ to be compared with the nucleon ground state where $\omega_0 = 2.04$, $R = 1.71$ fm, $M = 938$ MeV, and $D = -1.145$. Thin lines: asymptotic results for the bag model densities from Eq. (48) for $\sum \omega_j = 3\omega_{15}$ and R as given by Eq. (40).

where R is defined in Eq. (40) and it is understood that all quantities actually depend on a set of three (or two) values of ω_j for a higher baryonic (or mesonic) excitation. Except for the small-r region, the asymptotic expressions yield a good description of the gross features of the exact densities as shown in Fig. 6.

Remarkably, the asymptotic expression for $T_{00}(r)$ integrates to the exact expression for the baryon mass in Eq. (40). The asymptotic expressions for pressure and shear forces satisfy the differential equation (6), and $p(r)_{asymp}$ complies with the von Laue condition albeit not with its lower-dimensional analogs in (34) where the exact small-r details are essential. The asymptotic normal force $r^2[\frac{2}{3}s(r) + p(r)]_{asymp} = (\sum_j \omega_j)(1 - r^2/R^2)/(4\pi R^2)\Theta_V > 0$ for $r < R$ and vanishes at $r = R$. The two equivalent expressions in Eq. (7) yield the same asymptotic result for the D-term

$$D_{asymp} = -\frac{16}{135}\left(\sum_j \omega_j\right)^2. \qquad (49)$$

The energy mean square radius and mechanical radius are $\langle r_E^2 \rangle_{asymp} = \frac{2}{5}R^2$ and $\langle r_{mech}^2 \rangle_{asymp} = \frac{1}{5}R^2$. Finally, by exploring Eq. (40), we may eliminate the sum $\sum_j \omega_j$ in (49) in favor of M which yields (for mesons and baryons)

$$D_{asymp} = -AM^{8/3} \qquad (50)$$

with $A = \frac{1}{5}(16\pi\sqrt{3}B)^{-2/3}$. This asymptotic expression explains the strong rise of D with the mass observed in Fig. 5 where Eq. (50) is depicted as solid line. Interestingly the spectrum of radial Q-ball excitations exhibits the same asymptotic relation: for the Nth excitation the Q-ball mass grows like $M \propto N^3$ and D-term as $D \propto -N^8$, such that $D \propto -M^{8/3}$ [35] like in bag model. But the internal structure of the excitations is much different: e.g., the $p(r)$ of the Nth excited Q-ball state exhibits $(2N + 1)$ [35],

while the $p(r)$ of excited bag states have always only one node.

To end this section we comment on the near-degeneracies visible in Fig. 5 where the first 4000 states in the $J^P = \frac{1}{2}^+$ sector appear to be organized in a far smaller set of near-degenerate multiplets. To understand these near-degeneracies we notice that $\omega_j \approx (j + 3/4)\pi$ for $j \gtrsim 1$ can be further simplified[1] as $\omega_j \approx j\pi$ for large enough $j \gg 1$. If always all three occupied levels j_1, j_2, j_3 complied with this condition then the mass would be determined by three integers as $M \approx \text{const}(j_1 + j_2 + j_3)^{3/4}$ and the nth energy level would be $\frac{1}{2}n(n + 1)(n + 2)$–fold degenerated (like 3D harmonic oscillator formulated in Cartesian coordinates). Since for lower bag levels $j \gg 1$ is of course not valid, in practice a lesser degeneracy pattern is realized in Fig. 5.

VII. LIMITING CASES

In this section, we assume that $mR \neq 0$. The lowest solution ω_0 of the transcendental equation (12) depends on the product mR. We will be especially interested in the limit $\varepsilon = 1/(mR) \to 0$ where we have $\omega_0 \to \pi$. For our calculation the ε-corrections to ω_0 are essential. These corrections can be determined analytically, and are given by

$$\omega_0 = \pi - \frac{\pi}{2}\varepsilon + \frac{\pi^3}{6}\varepsilon^3 - \frac{7\pi^4}{48}\varepsilon^4 + \frac{\pi^3}{2}\left(\frac{1}{16} - \frac{\pi^2}{5}\right)\varepsilon^5$$
$$+ \frac{109\pi^5}{480}\varepsilon^6 + \mathcal{O}(\varepsilon^7), \quad \text{for } \varepsilon = \frac{1}{mR} \ll 1. \qquad (51)$$

---

[1]When deriving the asymptotic expressions for EMT densities (48), it is necessary to use the asymptotic solutions $\omega_j \to (j + 3/4)\pi$ of Eq. (12). Once we deal with the integrated quantities like M and D in (40) and (49), one may go one step further and approximate $\omega_j \to j\pi$ for $j \gg 1$. But we stress that this further simplification could not be used in the derivation of the asymptotic EMT densities (48).

After exploring the virial theorem for $m \neq 0$ in Eq. (A6) of Appendix, the bag constant becomes

$$B = \frac{N_c}{4R^3}\kappa(\varepsilon + \mathcal{O}(\varepsilon^2)), \qquad \kappa = \frac{\pi}{R}, \qquad c_0 = \frac{\pi}{2R^3}, \tag{52}$$

where we also define a constant c_0 which will be used in the subsequent equations. For the EMT densities, we obtain in the region $0 \leq r \leq R$ for $\varepsilon \ll 1$ the results

$$T_{00}(r) = N_c m c_0 j_0(\kappa r)^2 + \cdots,$$

$$\rho_J(r) = \frac{1}{3} c_0 \kappa r j_0(\kappa r) j_1(\kappa r) + \cdots,$$

$$s(r) = \frac{N_c \kappa}{2m} c_0 \left(-j_0'(\kappa r) j_1(\kappa r) - \frac{1}{r} j_0(\kappa r) j_1(\kappa r) + j_0(\kappa r) j_1'(\kappa r) \right) + \cdots,$$

$$p(r) = \frac{N_c \kappa}{6m} c_0 \left(-j_0'(\kappa r) j_1(\kappa r) + \frac{2}{r} j_0(\kappa r) j_1(\kappa r) + j_0(\kappa r) j_1'(\kappa r) \right) - \frac{N_c \kappa}{4mR^4}, + \cdots, \tag{53}$$

where the dots indicate subleading terms. For $r > R$, the densities are zero due to the Θ_V not shown here for brevity. Notice that $T_{00}(r) = \mathcal{O}(\varepsilon^{-1})$ and the dots indicate terms of $\mathcal{O}(\varepsilon^0)$ and $\rho_J(r) = \mathcal{O}(\varepsilon^0)$ and the dots indicating terms of $\mathcal{O}(\varepsilon)$, while $p(r)$ and $s(r)$ are both of $\mathcal{O}(\varepsilon)$ with dots indicating terms of $\mathcal{O}(\varepsilon^2)$.

Integrating $T_{00}(r)$ in (53) over the volume yields

$$M_N = \frac{N_c}{R} \left(\varepsilon^{-1} + \frac{5}{6}\pi^2 \varepsilon + \mathcal{O}(\varepsilon^2) \right)$$

$$= N_c m \left(1 + \frac{5}{6}\pi^2 \varepsilon^2 + \ldots \right). \tag{54}$$

The term of $\mathcal{O}(\varepsilon^0)$ contributing to $T_{00}(r)$ in (53) integrates exactly to zero, and the limit $M_N = N_c m$ is approached from above, i.e., with positive $\mathcal{O}(\varepsilon)$ corrections. Integrating $\rho_J(r)$ in (53) over the volume yields the nucleon spin $\int d^3 \rho_J(r) = \frac{1}{2}$ up to the order at which the expansion (51) of ω_0 is truncated [if one does not expand, the exact expression for $\rho_J(r)$ integrates of course to $\frac{1}{2}$ "to all orders"]. The pressure and shear forces in (53) comply with the von Laue condition and the lower dimensional conditions in (34) also up to the order at which the expansion of ω_0 in (51) is truncated (and are of course also valid to all orders if we do not expand).

Notice that the virial theorem is always valid as long as $\varepsilon \neq 0$. In the expansions in (53), the connection to the virial theorem is not visible. The leading term in $M_N = N_c m + \cdots$ is irrelevant for the virial theorem and drops out from $M_N'(R)$. Stability, pressure, and the von Laue condition are all encoded in the subsubleading terms of $\mathcal{O}(\varepsilon)$ in $T_{00}(r)$ in (53). This explains why the energy density is of $\mathcal{O}(\varepsilon^{-1})$ but the pressure and shear forces are of $\mathcal{O}(\varepsilon)$.

Using the expansion for $p(r)$ and $s(r)$ in (53), we obtain from (7) the result

$$D = -N_c^2 \left(\frac{4\pi^2 - 15}{45} - \frac{2\pi^2}{15}\varepsilon + \mathcal{O}(\varepsilon^2) \right). \tag{55}$$

The limit of the D-term in Eq. (55) applies to three different situations,

(i) $R = $ fixed, $\qquad m \to \infty,$

(ii) $m = $ fixed, $\qquad R \to \infty,$

(iii) $m \to \frac{1}{3}M_N, \qquad R \to \infty, \qquad M_N = $ fixed, $\qquad$ (56)

to be discussed below. The limits (i) and (ii) are briefly discussed in Ref. [80]. Figure. 7(a)–7(c) show how m, R, M_N are correlated in those limits. Figures 7(d)–7(f) show the behavior of the D-term.

The case (i) in (56) corresponds to the "heavy quark limit" where the nucleon mass $M_N \to N_c m$ becomes large; see Fig. 7(a). For $m \gtrsim 1$ GeV, we have $M_N \approx N_c m$ with a 10% or better accuracy. The asymptotics $M_N = N_c m$ is shown as dashed line in Fig. 7(a). This is intuitively expected; in the heavy quark limit, one expects that hadron masses are largely due to the heavy quark mass. In this limit, the quarks become "nonrelativistic"; it is $\alpha_+ = \mathcal{O}(\varepsilon^0)$, while $\alpha_- = \mathcal{O}(\varepsilon)$ such that the upper component of the spinor (11) dominates and the lower component goes to zero. Interestingly, the D-term is proportional to $\alpha_+\alpha_-$, see Eq. (37), but does not vanish because $M_N \propto \varepsilon^{-1}$ also enters its definition; see Eq. (7). Thus, $D \propto M_N\alpha_+\alpha_-$ has a nonzero limit; see (55). In Fig. 7(d), we show how the D-term changes as one varies the quark mass from $m = 0$ up to 1 TeV, with the asymptotic result (55) shown as a dashed line.

In the limit (ii) in (56), the boundary is moved to infinity for fixed m chosen to be 5 MeV in Fig. 7(b). Intuitively, one would expect to recover "free quarks" as the boundary is moved farther and farther away and the system becomes
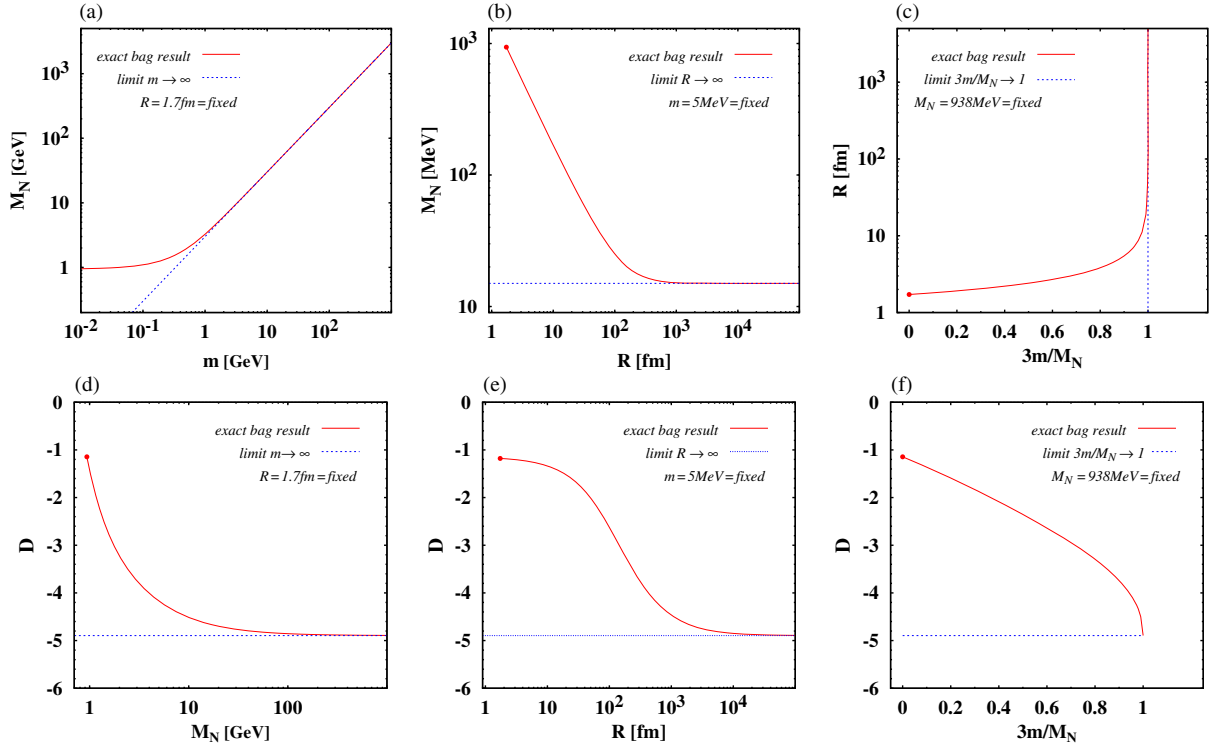
FIG. 7. (a) M_N as function of quark mass m for fixed $R = 1.7$ fm. (b) M_N as function of bag radius R for fixed $m = 5$ MeV. (c) R vs m (in units of $\frac{1}{3} M_N$) for fixed $M_N = 938$ MeV. (d) The D-term vs M_N for fixed $R = 1.7$ fm. (e) The D-term vs R for a fixed $m = 5$ MeV. (f) The D-term vs m (in units of $\frac{1}{3} M_N$) for fixed $M_N = 938$ MeV. The "physical point" with $M_N = 938$ MeV, $R = 1.7$ fm is marked [this point corresponds to $m = 5$ MeV in (b) and (d) and zero elsewhere].

more and more loosely bound. Indeed, also here $M_N \to N_c m$ [though in contrast to limit (i) the quarks may still be relativistic since m does not need to be large as long as it is nonzero]. This limit is approached from above according to Eq. (54) as shown in Fig. 7(b) where R is varied from 1.7 fm up to 1 Å with the asymptotic result $M_N = N_c m$ shown as a dashed line. Also in this limit, the D-term approaches the asymptotic value (55) as shown in Fig. 7(e). Remarkably, the D-term of a free fermion is zero [80], but here we do *not* recover this result, even though we deal with a more and more loosely bound system. The reason is as follows. As R becomes large, the "confinement" of the fermions inside an increasingly large cavity becomes less and less important, and the mass of the bound state approaches $M_N \to N_c m$. But no matter how small the "residual interactions" in an increasingly large cavity are, they remain nonzero, enter the description of the internal shear and pressure forces, and generate a nonzero D-term. How this happens can be traced back on the technical level through, for instance, the virial theorem; see Appendix. To recover a free theory, one has to take the limit $R \to \infty$ much earlier, on the Lagrangian level in Eq. (8) [80].

The limit (iii) in (56) is also very interesting. Here, we assume throughout a system with the fixed (physical) value of the nucleon mass, but we allow the model parameters m, R to vary such that the internal model dynamics interpolates

all the way from highly relativistic ($m = 0$) to highly nonrelativistic ($m \to \frac{1}{3} M_N$). In the bag model, the physical situation is of course more realistically reproduced for highly relativistic quarks rather than for nonrelativistic ones. But it is insightful to investigate such a transition from a highly to nonrelativistic system within a quark model. A convenient measure for this transition is m expressed in units of $\frac{1}{3} M_N$, i.e., the variable $3m/M_N$ of which the range is $0 \leq 3m/M_N \leq 1$. When $3m/M_N \to 0$, we deal with highly relativistic (massless) quarks in a relatively small system of radius $R = 1.7$ fm which corresponds to the "physical situation" in this model. When $3m/M_N \to 1$, we deal with a truly nonrelativistic model of the nucleon: in this limit, the nucleon mass is 100% due to the "constituent quark mass." In order to maintain in this limit the fixed (physical) value of the nucleon mass (in a system where the mass of the bound state is nearly entirely due to the mass of its constituents), it is necessary that the system becomes more loosely bound, which implies that the size of the system must increase. In the strict limit $m \to \frac{1}{3} M_N$, the bag radius diverges. The connection of m (in units of $\frac{1}{3} M_N$) and R for fixed $M_N = 938$ MeV is shown in Fig. 7(c). For instance, if we wanted 99.999% of nucleon mass to be due to the constituent quark masses, then $R = 0.57$ μm would be required. It should be stressed that, while

the system becomes more loosely bound in the sense that the binding energy decreases, we nevertheless still have confinement (in the specific way it is modeled in the bag model; it should be kept in mind that the binding energy is positive in a confining system). Since in the limit (iii) it is $m \to \frac{1}{3} M_N$ while $R \to \infty$, the D-term is again given by the limit $mR \to \infty$ quoted in Eq. (55). How the D-term behaves during the transition from a highly relativistic $(3m/M_N = 0)$ to a highly nonrelativistic $(3m/M_N \to 1)$ system with fixed M_N is shown in Fig. 7(f). For the last point included in this figure, it is $M_N - 3m = 10$ eV and $R = 4$ Å, which are numbers natural for systems in atomic physics.

The way the limiting value (55) of the D-term is approached in Figs. 7(d)–7(f) is characteristic for the three different limits in (56). When we plot D as function mR, the results from Figs. 7(d)–7(f) are in all three cases on a single universal curve shown in Fig. 8. Since D is dimensionless. it can only depend on the bag model parameters m and R in terms of the dimensionless variable mR. It is shown in Fig. 8 how the D-term depends on this dimensionless variable mR. The "physical situation" for the proton corresponds to the limit $mR \to 0$ (fixed $R = 1.7$ fm and light or massless up- and down-quarks). The limit $mR \to \infty$ can refer to the three different limiting cases in (56) discussed above.

One limiting case remains to be mentioned: fixed m and $R \to 0$. In this limit, one obtains a "pointlike" particle of which the mass diverges as $M_N \propto \frac{1}{R}$. This divergence is analogous to the difficulties associated with the description of pointlike particles or pointlike electric charges in classical physics. The description of the "internal structure" in a "pointlike particle" is of no immediate interest. We therefore refrain from discussing this limit further. The result for the D-term in this peculiar limit is, however, also shown in Fig. 8 in the direction $mR \to 0$.
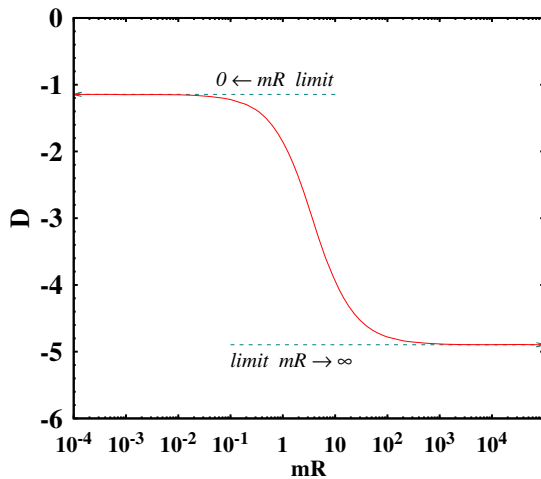

FIG. 8.   The D-term vs mR in the bag model. As a dimensionless quantity, the D-term only depends on the bag model parameters m and R through the dimensionless variable mR.

VIII. COUNTEREXAMPLE BOGOLIUBOV MODEL

In all theoretical approaches so far, the D-terms of particles were found negative, except for free fermion fields where $D = 0$ [80]. It is an interesting question whether positive D-terms can be realized at all in a physical system.

In fact, positive D-terms were found for *unphysical* states with spin and isospin $S = I \geq \frac{5}{2}$ in the rigid rotator approach in the Skyrme model [23]. Hadronic states with such ("exotic") quantum numbers are artifacts of the rigid rotator approach and not realized in nature. When computing masses and other properties of such states, one notices nothing unusual. But a more careful investigation of the EMT densities reveals why these states are unphysical: they do not obey the basic mechanical stability criterion, namely the positivity of normal forces $\frac{2}{3} s(r) + p(r) > 0$. So, the rigid rotator states with $S = I \geq \frac{5}{2}$ have positive D-terms, but they are also unphysical [23].

Despite its simplicity and drawbacks, the bag model is from the point of view of mechanical stability a perfectly reasonable and theoretically consistent framework with a negative D-term. However, a model which in some sense may be viewed as a predecessor of the bag model [78], the model of Bogoliubov [79], is insightful in this respect. In a certain limit, the Bogoliubov model basically corresponds to the bag model except that the bag constant B is absent. The nucleon mass is given by $M_{N,\text{Bogo}} = 3\frac{\omega_0}{R}$, and for $R = 1.29$ fm, the physical value of the nucleon mass is reproduced. An interesting parameter-free prediction of the Bogoliubov model is that for massless quarks the ratio of Roper and nucleon masses $M_{\text{Roper}}/M_N = (2\omega_0 + \omega_1)/(3\omega_0) = 1.55$ is close to the experimental value 1.53, although in retrospect, this has to be considered a "happy coincidence" [78], because the model is actually ill defined.

One way to understand this is to notice that the nucleon mass $M_{N,\text{Bogo}} = 3\frac{\omega_0}{R}$ is determined by fixing the bag radius by hand and not by a dynamical calculation [78], unlike the minimization procedure in the bag model underlying the virial theorem; see Sec. VA and Appendix. (In the bag model, we have *two* free parameters, B and R, one of which is dynamically determined by the virial theorem, and the other can then be fixed to reproduce a chosen hadron mass.) In fact, it is not possible to minimize $M_{N,\text{Bogo}} = 3\frac{\omega_0}{R}$ of which the minimum occurs for $R \to \infty$ [78].

The EMT densities shown in Fig. 9 illustrate what goes wrong in this model. The results for $T_{00}(r)$, $\rho_J(r)$, and $s(r)$ in Figs. 9(a)–9(c) look very similar to the bag model results in Figs. 2(a)–2(c) and do not hint at anything unusual. They could in principle describe a consistent system: e.g., $\int d^3 r T_{00}(r)$ yields the physical nucleon mass, and $\int d^3 r \rho_J(r)$ yields the nucleon spin $\frac{1}{2}$. The inconsistency of the Bogoliubov model becomes apparent when we inspect the pressure distribution in Fig. 9(d): $p(r)$ exhibits no node, and hence cannot comply with the von Laue
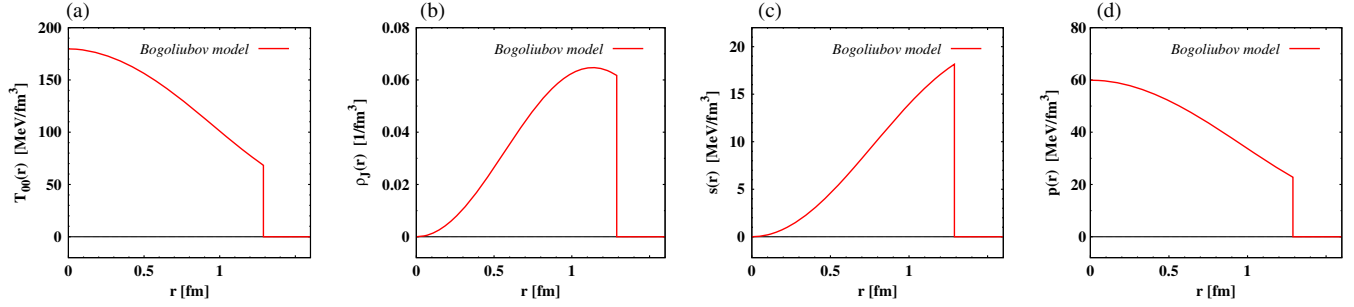
FIG. 9.　EMT densities as functions of r in the Bogoliubov model: (a) energy density $T_{00}(r)$, (b) angular momentum density $\rho_J(r)$, (c) shear forces $s(r)$, and (d) pressure $p(r)$. This version of the Bogoliubov model corresponds to the bag model with the bag constant B absent. The EMT densities are similar to the bag model except for the pressure which exhibits no node and does not comply with the von Laue condition, which means this is an inconsistent, unphysical solution.

condition in Eq. (34). Clearly, $\int_0^\infty dr\, r^2 p(r) > 0$ means that the internal forces are not compensated, and this solution actually "explodes." This is a consequence of fixing in this model the bag radius by hand [78]. In other words, there are no attractive forces in this model that would stabilize the solution at some finite radius (as it occurs in the bag model). Since the positive (repulsive) forces in the center of the nucleon are not compensated, the solution explodes; matter is dispersed all over the space. This corresponds to the observation that the "minimum" of $M_{N,\text{Bogo}}$ occurs only for $R \to \infty$ [78].

From the pressure distribution in Fig. 9(d), we would obtain a positive D-term by means of Eq. (7). It is interesting to remark that using the shear forces in Fig. 9(c) we, however, would obtain a negative D-term from Eq. (7). This mismatch persists even in the limit $R \to \infty$ and reflects the fact that the EMT is not conserved in this model. This is not surprising; the "by-hand fixing" of the bag radius corresponds to "external forces" which are imposed on the system but are not present in the Lagrangian. As a consequence, the dynamics is incomplete, and the EMT is not conserved. Equivalently, one may notice that, due to the absence of the bag constant, there is no form factor $\bar{c}^G(t)$ and the constraint $\sum_i \bar{c}^i(t) = 0$ is not satisfied.

To conclude this section, we notice that so far no consistent physical system has been found where the D-term would be positive. The excursion to the Bogoliubov model, which is nicely presented in the historical context in Ref. [78], has only revealed an example where a positive D-term is encountered due to an incomplete dynamical description of a system. One way to cure the inconsistencies of this model consists in introducing a bag constant. We have seen in the previous sections how, from the point of view of mechanical stability, this yields a consistent description.

IX. CONCLUSIONS

In this work, we have explored the bag model to study the EMT form factors $A^a(t)$, $J^a(t)$, $D^a(t)$, and $\bar{c}^a(t)$ and the EMT densities. The quark contributions ($a = u, d$) to the

EMT form factors are defined in terms of the single-quark wave functions and the SU(4) spin-flavor factors needed to construct the nucleon wave functions. The form factors $A^a(t)$, $J^a(t)$, and $D^a(t)$ receive only quark contributions; i.e., in these cases, the total form factors are given by $A(t) = A^u(t) + A^d(t)$ and analogously for $J(t)$ and $D(t)$. In principle, also the bag makes contributions to form factors which can be interpreted as gluonic contributions. Only the form factor $\bar{c}^a(t)$ receives such a gluonic contribution.

It is crucial to check that all relations derived from $\partial_\mu T^{\mu\nu} = 0$ are valid, and to demonstrate the mechanical stability of the model. The theoretical consistency is reflected in various ways. We have shown that the bag model description of the EMT form factors is consistent in the large-N_c limit. The constraints $A(0) = 1$ and $J(0) = \frac{1}{2}$ are satisfied, and $\sum_a \bar{c}^a(t) = 0$ holds for all t. Since the bag contribution is not described in terms of a wave function, it was necessary to determine the gluonic form factor $\bar{c}^G(t)$ using a different method by resorting to the EMT density formalism. The large-N_c formulation of the bag model correctly reproduces the general large-N_c counting rules for the EMT form factors [6]. The usage of the large-N_c limit has moreover the advantage of resolving technical problems associated with form factor calculations in independent-particle models like the bag model. When considering the large-N_c limit, our expressions for the EMT form factors agree with those from Ref. [10]. We have shown that the $1/N_c$ corrections associated with our large-N_c treatment of the EMT form factors are relatively small for $|t| \ll M_N$.

The large-N_c limit automatically provides a rigorous justification for the concept of 3D densities. We studied the energy density $T^{00}(r)$, the angular momentum density $J^i(\vec{r}) = \epsilon^{ijk} r^j T^{0k}(\vec{r})$, and the distributions of shear forces and pressure related to the stress tensor $T^{ij}(\vec{r})$. We have shown that the bag model EMT densities comply with all general requirements including the von Laue condition, which is a necessary condition for stability. The bag model also complies with analogous lower-dimensional stability

conditions. Another important result is that the angular momentum density $J^i(\vec{r})$ in the bag model can be decomposed in monopole and quadrupole terms which are model-independently related to each other.

We presented an extensive study of the D-term in the bag model, not only for the nucleon but also for other hadrons including $N^{\star}$-resonances, vector mesons, Δ-resonances, and hypothetical highly excited bag model states. We have shown that in all cases the D-term is negative. We made the interesting observation that asymptotically the D-terms grow as $D = -\text{const} \times M^{8/3}$ with the mass M of the excitation. Interestingly, the same asymptotic dependence was found for high excitations in the Q-ball system [35] even though the internal structure of the excited states in the two systems is much different; for instance, the pressure in the Nth excited state exhibits $(2N + 1)$-nodes in the Q-ball system but one and only one node in the bag model. We are not aware of whether the growth $D = -\text{const} \times M^{8/3}$ of the D-term with the mass M of the excitation is a general result or a common peculiarity of these two (very different) systems. It will be interesting to investigate this result in other theoretical systems. At this point, it is not known how to access information on the EMT form factors of N^* states, but information on transition form factors can in principle be deduced from studies of hard exclusive reactions. This field has a lot of potential.

The study of excited states has brought very interesting insights. For instance, while the mass increases by about 50% as one goes from the ground state (nucleon) to the first excited state (Roper), the internal pressure in the center and the D-term increase by factor 7. This finding supports the observations made in other systems that the D-term is a quantity which most strongly reflects the internal dynamics of the system and exhibits the strongest variations as one for instance considers higher excited states. The ground state and all excited states correspond to mininima of the action, and comply therefore with the necessary stability condition provided by the von Laue relation, and the D-terms are always negative. However, only the ground state is the global minimum of the action, and hence absolutely stable. The excited states correspond to local minima and can decay into the ground state.

We studied the D-term in three different limits: the heavy quark limit, large bag-radius limit, and nonrelativistic limit. The D-term assumes the same well-defined finite value in these three limits, which can be computed analytically. This shows that the D-term is a property of all systems including nonrelativistic systems. Since $D = 0$ for a free fermion [80], this also provides an illustration how e.g., even very small interactions in the bag model (in the limit of a very large bag radius) generate a nonzero D-term.

The bag model is at variance with chiral symmetry, and its oversimplified description cannot be expected to give accurate predictions. But one main goal of this work was to shed light on the interpretation of EMT form factors in terms of 3D densities. For this, it is crucial to use a consistent theoretical framework, and the bag model provides this. The simplicity of this model is a crucial advantage when elucidating the concepts. For instance, it was observed in several models that the von Laue condition $\int_0^\infty dr\, r^2 p(r) = 0$ is related to the virial theorem. This is also the case in the bag model, and we were able to show that not only this but also the lower-dimensional analogs of the von Laue condition are satisfied provided one works with a solution satisfying the virial theorem. Another interesting observation is related to the mechanical stability requirement that the normal force per unit area $\frac{2}{3} s(r) + p(r) \geq 0$. This quantity is positive inside the bag, and the point where it drops to zero marks the "edge of the system," i.e., the bag boundary in our case. Such an observation can only be obtained in a finite size system.

Finally, we studied the EMT densities in the Bogoliubov model [79], a predecessor of the bag model in which the bag contribution is absent and the bag radius needs to be fixed by hand. This model provides a counterexample for a framework where the nucleon is not consistently described. Fixing the bag radius by hand (rather than by means of a dynamical equation) corresponds to external forces which are not included in the Lagrangian. This implies an unphysical situation in which the EMT is not conserved and where the pressure has no node and the von Laue condition is not satisfied. From such a positive pressure, one would obtain an unphysical positive D-term. This problem is solved in the bag model by introducing a nonzero bag constant B in the Lagrangian.

It will be interesting to study the EMT form factors and the associated densities in other models of which the nature is classical, quantum mechanical, or field theoretical. Such studies deepen our understanding of the hadron structure.

ACKNOWLEDGMENTS

APPENDIX: TECHNICAL DETAILS AND PROOFS

This Appendix contains technical details. Let us quote first the expressions for the first three spherical Bessel functions

$$j_0(x) = \frac{\sin x}{x}, \qquad j_1(x) = \frac{\sin x}{x^2} - \frac{\cos x}{x},$$

$$j_2(x) = 3\frac{\sin x}{x^3} - 3\frac{\cos x}{x^2} - \frac{\sin x}{x}. \tag{A1}$$

Below, we shall also make use of the expansion of a plane wave $e^{i\vec{\Delta}\vec{r}}$ in terms of spherical Bessel functions and Legendre polynomials $P_l(x)$ as well as the orthogonality relation of the latter,

$$e^{i\vec{q}\vec{r}} = \sum_{l=0}^{\infty} i^l (2l+1) j_l(qr) P_l(\cos\theta),$$

$$\int_{-1}^{1} d\cos\theta P_l(\cos\theta) P_k(\cos\theta) = \frac{2}{2l+1}\delta_{lk}. \quad (A2)$$

In order to abbreviate the expressions below, let us define the integrals over the combinations of spherical Bessel functions entering respectively the expressions for $p(r)$ and $s(r)$, namely

$$I_n^p(\omega) = \int_0^\omega dx\, x^n \left(j_0(x)j_1'(x) - j_0'(x)j_1(x) + \frac{2}{x}j_0(x)j_1(x) \right),$$

$$I_n^s(\omega) = \int_0^\omega dx\, x^n \left(j_0(x)j_1'(x) - j_0'(x)j_1(x) - \frac{1}{x}j_0(x)j_1(x) \right).$$

$$(A3)$$

1. Virial theorem in general case

Let us generalize the virial theorem (26) to general (including excited) states with $m \neq 0$. In the general case, the mass of a hadron is obtained by occupying $N_{\rm const}$ energy levels $\varepsilon_i = \Omega_i/R$ and adding the energy due to the bag,

$$M(R) = \frac{1}{R}\sum_i \Omega_i + \frac{4\pi}{3}BR^3, \quad (A4)$$

where the sum goes over the occupied levels $i = 1,\ldots,N_{\rm const}$ and $N_{\rm const}$ denotes the number of constituents with $N_{\rm const} = 2$ for mesons and $N_{\rm const} = N_c$ for baryons.

The $\Omega_i = \sqrt{\omega_i^2 + m^2 R^2}$ depend on R explicitly and the ω_i implicitly through the transcendental equation (12). The derivative of ω_i with respect to R is determined by differentiating Eq. (12) with respect to R, which, upon exploring (12) to eliminate trigonometric functions, yields

$$\frac{\partial \omega_i}{\partial R} = \frac{m\omega_i}{2\Omega_i(\Omega_i - 1) + mR}. \quad (A5)$$

Using the result (A5), we obtain the virial theorem valid for $m \neq 0$ and excited states, which is given by

$$M_N'(R) = -\frac{1}{R^2}\sum_i \frac{2(\Omega_i - 1)\omega_i^2}{2\Omega_i(\Omega_i - 1) + mR} + 4\pi R^2 B \overset{!}{=} 0$$

$$\Leftrightarrow 4\pi R^4 B = \sum_i \frac{2(\Omega_i - 1)\omega_i^2}{2\Omega_i(\Omega_i - 1) + mR}. \quad (A6)$$

If one takes $m \to 0$, the derivative (A5) vanishes, and the virial theorem (A6) reduces to Eq. (26) for the nucleon.

2. Proof of von Laue condition

For notational convenience, we present the proof for the nucleon case. The generalization to other bag states is straightforward. Integrating $p(r)$ in Eq. (29) over d^3r and using the substitution $r \to x = \omega r/R$ yields

$$\int d^3r\, p(r) = N_c A^2 \alpha_+ \alpha_- \frac{R^2}{3\omega_0^2} I_2^p(\omega_0) - \frac{4\pi}{3}BR^3. \quad (A7)$$

The integral over the Bessel functions $I_2^p(\omega_0)$ is defined in Eq. (A3) and yields

$$I_2^p(\omega_0) = \frac{\omega_0^2 - \sin^2\omega_0}{\omega_0}. \quad (A8)$$

Inserting (A8) into Eq. (A7), we find

$$\int d^3r\, p(r) = N_c A^2 \alpha_+ \alpha_- \frac{R^2}{3\omega_0^2} \frac{\omega_0^2 - \sin^2\omega_0}{\omega_0} - \frac{4\pi}{3}BR^3 \overset{!}{=} 0.$$

$$(A9)$$

That Eq. (A9) is zero becomes apparent after inserting the expressions for A and $\alpha_\pm$ defined in the context of Eq. (11), exploring the transcendental equation (12) to eliminate trigonometric functions and some tedious algebra, which yields

$$\int d^3r\, p(r) = \frac{N_c}{3R} \frac{2\omega_0^2(\Omega_0 - 1)}{2\Omega_0(\Omega_0 - 1) + mR} - \frac{4\pi}{3}BR^3$$

$$= -\frac{1}{3}RM_N'(R) \overset{!}{=} 0, \quad (A10)$$

where in the second step we made use of the virial theorem (A6) for the nucleon case.

To prove the 2D analog of the von Laue condition, we consider

$$\int_0^\infty dr\, r\left(-\frac{1}{3}s(r) + p(r) \right)$$

$$= N_c \frac{A^2}{4\pi}\alpha_+\alpha_- \frac{R}{3\omega}[-I_1^s(\omega_0) + I_1^p(\omega_0)] - \frac{1}{2}BR^2$$

$$= -\frac{1}{8\pi}M_N'(R) \overset{!}{=} 0, \quad (A11)$$

where in the last step we used Eqs. (A6) and (A9). Similarly for the 1D version of the von Laue condition, we find

$$\int_0^\infty dr \left(-\frac{4}{3} s(r) + p(r) \right)$$

$$= N_c \frac{A^2}{4\pi} \alpha_+ \alpha_- \frac{1}{3} [-4I_0^s(\omega_0) + I_0^p(\omega_0)] - BR$$

$$= -\frac{1}{4\pi R} M_N'(R) \overset{!}{=} 0. \tag{A12}$$

Notice that the integrals $I_0^s(\omega_0)$, $I_0^p(\omega_0)$, $I_1^s(\omega_0)$, $I_1^p(\omega_0)$ are well defined but contain sine- and cosine-integral terms which cancel out in the linear combinations in the square brackets in (A11) and (A12). The results (A10), (A11), and (A12) show that the von Laue condition and its lower-dimensional analogs are all satisfied if the virial theorem is satisfied.

3. Equivalence of *D*-term expressions

In this section, let us distinguish the expressions D_p and D_s for the *D*-term in terms of pressure and shear forces as defined in Eq. (7). For D_p, we have

$$D_p = M_N \int d^3 r \, r^2 p(r)$$

$$= M_N \left(N_c A^2 \alpha_+ \alpha_- \frac{R^4}{3\omega_0^4} I_4^p(\omega_0) - \frac{4\pi}{5} BR^5 \right), \tag{A13}$$

where the integral over Bessel functions yields

$$I_4^p(\omega_0) = \frac{\omega_0^3}{3} + \omega_0 - \omega_0 \sin^2 \omega_0 - \sin \omega_0 \cos \omega_0. \tag{A14}$$

Exploring the expression (A9) for the von Laue condition to eliminate *B* yields

$$D_p = M_N N_c A^2 \alpha_+ \alpha_- \frac{R^4}{3\omega_0^4} \left(-\frac{4}{15} \omega_0^3 + \omega_0 \right.$$

$$\left. -\frac{2}{5} \omega_0 \sin^2 \omega_0 - \sin \omega_0 \cos \omega_0 \right) \tag{A15}$$

and corresponds to the expression quoted in Eq. (37).

To show that the expression in terms of shear forces yields the same result, we consider

$$D_s = -\frac{4}{15} M_N \int d^3 r \, r^2 s(r)$$

$$= -\frac{4}{5} M_N N_c A^2 \alpha_+ \alpha_- \frac{R^4}{3\omega_0^4} I_4^s(\omega_0) \tag{A16}$$

with the integral over Bessel functions given by

$$I_4^s(\omega_0) = \frac{\omega_0^3}{3} - \frac{5}{4} \omega_0 + \frac{5}{4} \sin \omega_0 \cos \omega_0 + \frac{1}{2} \omega_0 \sin^2 \omega_0. \tag{A17}$$

The difference of the two expressions for the *D*-term is

$$D_p - D_s = M_N N_c A^2 \alpha_+ \alpha_- \frac{R^4}{3\omega_0^4} \left(I_4^p(\omega_0) + \frac{4}{5} I_4^s(\omega_0) \right)$$

$$-\frac{4}{5} \pi M_N BR^5 = -\frac{1}{5} R^3 M_N M_N'(R) \overset{!}{=} 0, \tag{A18}$$

where in the last step we once more made use of Eqs. (A6) and (A9). This proves that the expressions for the *D*-term in terms of $p(r)$ and $s(r)$ are equivalent.

4. Proof that $\bar{c}^Q(t) + \bar{c}^G(t) = 0$

In the main text, it was shown that at $t = 0$ it is $\bar{c}^Q(0) + \bar{c}^G(0) = 0$. We now wish to generalize this proof to $t \neq 0$. The proof is elementary but tedious such that it is worth showing it in some more detail. The starting point is $\bar{c}^Q(t)$ in (23c). We recall that $\vec{k}' = \vec{k} + \vec{\Delta}$ with $\vec{\Delta} = (0, 0, \Delta^3)$ in our kinematics. The right-hand side of (23c) is an even function of Δ^3. To show this, we replace $\Delta^3 \to (-\Delta^3)$ and subsequently substitute $k^3 \to (-k^3)$, which restores the starting expression. This proves that $\bar{c}^Q(t)$ can be understood as a function of $t = -\vec{\Delta}^2$ as it must for a form factor. In the next step, we explore this to simplify the expression for $\bar{c}^Q(t)$ as follows. In the first term in the square brackets of (23c), we substitute $k^3 \to k^3 - \Delta^3$, and subsequently we explore that the function is even under $\Delta^3 \to (-\Delta^3)$, which restores the original expression but with $\vec{k}$ and $\vec{k}'$ exchanged. This allows us to write Eq. (23c) as

$$\bar{c}^Q(t) = -b \int \frac{d^3 k}{(2\pi)^3} (k'^3 + k^3) [t_0(k') t_1(k) e_k^3],$$

$$b = \frac{4\pi A^2 R^6 N_c}{M_N} \alpha_+ \alpha_-, \tag{A19}$$

where $\vec{e}_k = \vec{k}/k$. It is convenient to work in coordinate space. In the formulas below, Bessel functions j_l with no argument will denote $j_l(w_i r/R)$ for notational simplicity, and the primes will denote derivatives with respect to r. In order to avoid total derivatives (which in general do not vanish in the finite volume integrals in the bag model and cause a proliferation of terms), we proceed by introducing a δ-function as follows:

$$\bar{c}^Q(t) = -b \left[\int \frac{d^3 k}{(2\pi)^3} t_0(k) k^3 \int \frac{d^3 q}{(2\pi)^3} t_1(q) e_q^3 \right.$$

$$\left. + \int \frac{d^3 k}{(2\pi)^3} t_0(k) \int \frac{d^3 q}{(2\pi)^3} t_1(q) q^3 e_q^3 \right] \int d^3 r \, e^{i\vec{r}(\vec{k} - \vec{q})}. \tag{A20}$$

In the next step, we invert the Fourier transforms, where $\Theta_V = \Theta(R - r)$ is used for brevity and we use identities

$$\int \frac{d^3 q}{(2\pi)^3} t_0(q) e^{i\vec{r}\vec{q}} = j_0 \frac{\Theta_V}{4\pi R^3}, \qquad \int \frac{d^3 q}{(2\pi)^3} \vec{e}_q t_1(q) e^{-i\vec{r}\vec{q}} = -i\vec{e}_r j_1 \frac{\Theta_V}{4\pi R^3}, \tag{A21}$$

where (as before) $j_i = j_i(\omega r/R)$ for brevity. This yields

$$\bar{c}^Q(t) = \frac{b}{(4\pi R^3)^2} \int d^3 r\, e^{i\vec{r}\vec{\Delta}} \left[(e_r^3)^2 \left(j_0' j_1 - j_0 j_1' + \frac{j_0 j_1}{r} \right) - \frac{j_0 j_1}{r} \right] \Theta_V. \tag{A22}$$

Finally, we explore that $e_r^3 = \vec{e}_z \cdot \vec{e}_r = \cos\theta$ such that $(e_r^3)^2 = \frac{2}{3} P_2(\cos\theta) + \frac{1}{3} P_0(\cos\theta)$. Making use of the expansion of $e^{i\vec{r}\vec{\Delta}}$ and the orthogonality of Legendre polynomials in (A2), we obtain

$$\bar{c}^Q(t) = \frac{b}{(4\pi R^3)^2} \int_V d^3 r \left[\underbrace{\left(-\frac{2}{3} j_2(\Delta r) + \frac{1}{3} j_0(\Delta r) \right)}_{\frac{1}{\Delta} j_1'(\Delta r)} (j_0' j_1 - j_0 j_1') + \underbrace{\left(-\frac{1}{3} j_2(\Delta r) - \frac{1}{3} j_0(\Delta r) \right)}_{=-\frac{j_1(\Delta r)}{\Delta r}} \frac{2 j_0 j_1}{r} \right], \tag{A23}$$

where the underbraces indicate useful identities. Another helpful identity is $2 j_0 j_1 = -\frac{\partial}{\partial r}[r^2 (j_0' j_1 - j_0 j_1')]$. After integrating over the solid angle, we find that the r-integrand is a total derivative,

$$\bar{c}^Q(t) = \frac{4\pi b}{(4\pi R^3)^2 \Delta} \int_0^R dr \left[\frac{\partial}{\partial r}[j_1(\Delta r) r^2 (j_0' j_1 - j_0 j_1')] \right] = -c_0 \frac{j_1(\Delta R)}{\Delta R}. \tag{A24}$$

In the massless case, the prefactor c_0 is given by

$$c_0 = \frac{b}{4\pi R^3} \frac{\omega_0}{R} (j_0(\omega_0) j_1'(\omega_0) - j_0'(\omega_0) j_1(\omega_0)) = \frac{3}{4}, \tag{A25}$$

which follows from using the transcendental equation (12). In the massive case, the result is a different fraction, and the last step is lengthier, and one has to use the expression for B from the massive virial theorem to show that the constraint $\sum_i \bar{c}^i(t)$ holds also here.

5. EMT form factor of the antisymmetric EMT

For completeness, we discuss the form factors of the canonical EMT defined by $T_{\text{can}}^{\mu\nu,q} = \frac{1}{2}\bar{\psi}_q(-i\gamma^\mu \overleftarrow{\partial}^\nu + i\gamma^\mu \overrightarrow{\partial}^\nu)\psi_q$. The canonical EMT can be decomposed in two parts: a symmetric part of which the form factors $A^q(t)$, $J^q(t)$, $D^q(t)$, and $\bar{c}^q(t)$ were discussed in the main text and an antisymmetric part which is characterized by a single form factor [100]

$$\langle p'| \frac{1}{2} (\hat{T}_{\text{can}}^{\mu\nu,q}(0) - \hat{T}_{\text{can}}^{\nu\mu,q}(0))|p\rangle = F_{\text{can}}^q(t) \bar{u}(p') \frac{i(P^\mu \sigma^{\nu\rho} - P^\nu \sigma^{\mu\rho})\Delta_\rho}{4 M_N} u(p), \tag{A26}$$

which in the bag model is given by

$$F_{\text{can}}^q(t) = 4\pi A^2 R^6 \int \frac{d^3 k}{(2\pi)^3} \left[2\alpha_+ \alpha_- \frac{\varepsilon_0}{\Delta^3} \left(t_0(k') t_1(k) \frac{k^3}{k} - t_0(k) t_1(k') \frac{k'^3}{k'} \right) + k_\perp^2 \alpha_-^2 \frac{t_1(k)}{k} \frac{t_1(k')}{k'} \right]. \tag{A27}$$

The expression (A27) agrees up to the sign with the bag model results for the axial form factor $G_A^q(t)$. Thus, we recover $F_{\text{can}}^q(t) = -G_A^q(t)$, which is a model-independent result [100]. This shows that also the canonical EMT is consistently described within the bag model.

[1] I. Y. Kobzarev and L. B. Okun, Zh. Eksp. Teor. Fiz. **43**, 1904 (1962) [Sov. Phys. JETP **16**, 1343 (1963)]; H. Pagels, Phys. Rev. **144**, 1250 (1966).

[2] D. Müller, D. Robaschik, B. Geyer, F.-M. Dittes, and J. Hořejši, Fortschr. Phys. **42**, 101 (1994).

[3] X. D. Ji, Phys. Rev. Lett. **78**, 610 (1997); Phys. Rev. D **55**, 7114 (1997).

[4] A. V. Radyushkin, Phys. Lett. B **380**, 417 (1996); **385**, 333 (1996); Phys. Rev. D **56**, 5524 (1997).

[5] J. C. Collins, L. Frankfurt, and M. Strikman, Phys. Rev. D **56**, 2982 (1997).

[6] K. Goeke, M. V. Polyakov, and M. Vanderhaeghen, Prog. Part. Nucl. Phys. **47**, 401 (2001).

[7] M. Diehl, Phys. Rep. **388**, 41 (2003); A. V. Belitsky and A. V. Radyushkin, Phys. Rep. **418**, 1 (2005); S. Boffi and B. Pasquini, Riv. Nuovo Cimento **30**, 387 (2007).

[8] M. V. Polyakov, Phys. Lett. B **555**, 57 (2003).

[9] M. V. Polyakov and P. Schweitzer, Int. J. Mod. Phys. A **33**, 1830025 (2018).

[10] X. D. Ji, W. Melnitchouk, and X. Song, Phys. Rev. D **56**, 5511 (1997).

[11] V. Y. Petrov, P. V. Pobylitsa, M. V. Polyakov, I. Börnig, K. Goeke, and C. Weiss, Phys. Rev. D **57**, 4325 (1998).

[12] P. Schweitzer, S. Boffi, and M. Radici, Phys. Rev. D **66**, 114004 (2002).

[13] J. Ossmann, M. V. Polyakov, P. Schweitzer, D. Urbano, and K. Goeke, Phys. Rev. D **71**, 034011 (2005).

[14] M. Wakamatsu and H. Tsujimoto, Phys. Rev. D **71**, 074001 (2005).

[15] M. Wakamatsu and Y. Nakakoji, Phys. Rev. D **74**, 054006 (2006).

[16] K. Goeke, J. Grabis, J. Ossmann, M. V. Polyakov, P. Schweitzer, A. Silva, and D. Urbano, Phys. Rev. D **75**, 094021 (2007).

[17] K. Goeke, J. Grabis, J. Ossmann, P. Schweitzer, A. Silva, and D. Urbano, Phys. Rev. C **75**, 055207 (2007).

[18] M. Wakamatsu, Phys. Lett. B **648**, 181 (2007).

[19] C. Cebulla, K. Goeke, J. Ossmann, and P. Schweitzer, Nucl. Phys. **A794**, 87 (2007).

[20] H. C. Kim, P. Schweitzer, and U. Yakhshiev, Phys. Lett. B **718**, 625 (2012).

[21] J. H. Jung, U. Yakhshiev, and H. C. Kim, J. Phys. G **41**, 055107 (2014).

[22] J. H. Jung, U. Yakhshiev, H. C. Kim, and P. Schweitzer, Phys. Rev. D **89**, 114021 (2014).

[23] I. A. Perevalova, M. V. Polyakov, and P. Schweitzer, Phys. Rev. D **94**, 054024 (2016).

[24] Z. Abidin and C. E. Carlson, Phys. Rev. D **77**, 095007 (2008).

[25] Z. Abidin and C. E. Carlson, Phys. Rev. D **77**, 115021 (2008).

[26] S. J. Brodsky and G. F. de Teramond, Phys. Rev. D **78**, 025032 (2008).

[27] Z. Abidin and C. E. Carlson, Phys. Rev. D **79**, 115003 (2009).

[28] K. A. Mamo and I. Zahed, arXiv:1910.04707.

[29] E. Megias, E. Ruiz Arriola, L. L. Salcedo, and W. Broniowski, Phys. Rev. D **70**, 034031 (2004).

[30] E. Megias, E. Ruiz Arriola, and L. L. Salcedo, Phys. Rev. D **72**, 014001 (2005).

[31] W. Broniowski and E. R. Arriola, Phys. Rev. D **78**, 094011 (2008).

[32] N. Kumar, C. Mondal, and N. Sharma, Eur. Phys. J. A **53**, 237 (2017).

[33] D. Chakrabarti, C. Mondal, and A. Mukherjee, Phys. Rev. D **91**, 114026 (2015).

[34] M. Mai and P. Schweitzer, Phys. Rev. D **86**, 076001 (2012).

[35] M. Mai and P. Schweitzer, Phys. Rev. D **86**, 096002 (2012).

[36] M. Cantara, M. Mai, and P. Schweitzer, Nucl. Phys. **A953**, 1 (2016).

[37] I. E. Gulamov, E. Y. Nugaev, A. G. Panin, and M. N. Smolyakov, Phys. Rev. D **92**, 045011 (2015).

[38] E. Nugaev and A. Shkerin, arXiv:1905.05146.

[39] J. Hudson and P. Schweitzer, Phys. Rev. D **96**, 114013 (2017).

[40] A. Freese and I. C. Cloët, Phys. Rev. C **100**, 015201 (2019).

[41] A. Freese and I. C. Cloët, arXiv:1907.08256.

[42] A. V. Belitsky and X. Ji, Phys. Lett. B **538**, 289 (2002).

[43] S. I. Ando, J. W. Chen, and C. W. Kao, Phys. Rev. D **74**, 094013 (2006).

[44] M. Diehl, A. Manashov, and A. Schäfer, Eur. Phys. J. A **29**, 315 (2006).

[45] P. Masjuan, E. Ruiz Arriola, and W. Broniowski, Phys. Rev. D **87**, 014005 (2013).

[46] B. Pasquini, M. V. Polyakov, and M. Vanderhaeghen, Phys. Lett. B **739**, 133 (2014).

[47] N. Mathur, S. J. Dong, K. F. Liu, L. Mankiewicz, and N. C. Mukhopadhyay, Phys. Rev. D **62**, 114504 (2000).

[48] P. Hägler, J. W. Negele, D. B. Renner, W. Schroers, T. Lippert, and K. Schilling (LHPC and SESAM Collaborations), Phys. Rev. D **68**, 034505 (2003); M. Göckeler, R. Horsley, D. Pleiter, P. E. L. Rakow, A. Schäfer, G. Schierholz, and W. Schroers (QCDSF Collaboration), Phys. Rev. Lett. **92**, 042002 (2004).

[49] P. Hägler *et al.* (LHPC Collaboration), Phys. Rev. D **77**, 094502 (2008).

[50] P. E. Shanahan and W. Detmold, Phys. Rev. D **99**, 014511 (2019); Phys. Rev. Lett. **122**, 072003 (2019).

[51] I. V. Anikin, Phys. Rev. D **99**, 094026 (2019); K. Azizi and U. Özdem, arXiv:1908.06143.

[52] I. R. Gabdrakhmanov and O. V. Teryaev, Phys. Lett. B **716**, 417 (2012).

[53] S. Friot, B. Pire, and L. Szymanowski, Phys. Lett. B **645**, 153 (2007).

[54] M. V. Polyakov and C. Weiss, Phys. Rev. D **60**, 114017 (1999).

[55] O. V. Teryaev, Phys. Lett. B **510**, 125 (2001).

[56] S. Kumano, Q. T. Song, and O. V. Teryaev, Phys. Rev. D **97**, 014020 (2018).

[57] V. D. Burkert, L. Elouadrhiri, and F. X. Girod, Nature (London) **557**, 396 (2018).

[58] K. Kumerički, Nature (London) **570**, E1 (2019).

[59] A. Chodos, R. L. Jaffe, K. Johnson, C. B. Thorn, and V. F. Weisskopf, Phys. Rev. D **9**, 3471 (1974).

[60] A. Chodos, R. L. Jaffe, K. Johnson, and C. B. Thorn, Phys. Rev. D **10**, 2599 (1974).

[61] T. A. DeGrand, R. L. Jaffe, K. Johnson, and J. E. Kiskis, Phys. Rev. D **12**, 2060 (1975).

[62] R. L. Jaffe, Phys. Rev. D **11**, 1953 (1975).

[63] L. S. Celenza and C. M. Shakin, Phys. Rev. C **27**, 1561 (1983); **39**, 2477(E) (1989).

[64] R. L. Jaffe and X. D. Ji, Nucl. Phys. **B375**, 527 (1992).

[65] A. Courtoy, F. Fratini, S. Scopetta, and V. Vento, Phys. Rev. D **78**, 034002 (2008).

[66] H. Avakian, A. V. Efremov, P. Schweitzer, and F. Yuan, Phys. Rev. D **78**, 114024 (2008).

[67] H. Avakian, A. V. Efremov, P. Schweitzer, and F. Yuan, Phys. Rev. D **81**, 074035 (2010).

[68] H. M. Chang, A. V. Manohar, and W. J. Waalewijn, Phys. Rev. D **87**, 034009 (2013).

[69] M. Rinaldi, S. Scopetta, and V. Vento, Phys. Rev. D **87**, 114021 (2013).

[70] C. Lorcé, L. Mantovani, and B. Pasquini, Phys. Lett. B **776**, 38 (2018).

[71] P. Schweitzer and K. Tezgin, Phys. Lett. B **796**, 47 (2019).

[72] M. V. Polyakov and P. Schweitzer, arXiv:1801.05858.

[73] M. V. Polyakov and H. D. Son, J. High Energy Phys. 09 (2018) 156.

[74] C. Lorcé, H. Moutarde, and A. P. Trawiński, Eur. Phys. J. C **79**, 89 (2019).

[75] M. V. Polyakov and P. Schweitzer, Proc. Sci., SPIN2018 (**2019**) 066 [arXiv:1812.06143].

[76] M. V. Polyakov and B. D. Sun, Phys. Rev. D **100**, 036003 (2019).

[77] W. Cosyn, S. Cotogno, A. Freese, and C. Lorcé, Eur. Phys. J. C **79**, 476 (2019).

[78] A. W. Thomas and W. Weise, *The Structure of the Nucleon* (Wiley-VCH, Berlin, 2001), p. 389.

[79] P. N. Bogoliubov, Ann. Inst. Henri Poncaré **8**, 163 (1967).

[80] J. Hudson and P. Schweitzer, Phys. Rev. D **97**, 056003 (2018).

[81] M. J. Neubelt, A. Sampino, J. Hudson, K. Tezgin, and P. Schweitzer, Proc. Sci., DIS2019 (**2019**) 210 [arXiv:1907.11185].

[82] R. G. Sachs, Phys. Rev. **126**, 2256 (1962).

[83] P. Lowdon, K. Y. J. Chiu, and S. J. Brodsky, Phys. Lett. B **774**, 1 (2017).

[84] S. Cotogno, C. Lorcé, and P. Lowdon, Phys. Rev. D **100**, 045003 (2019).

[85] G. Karl and J. E. Paton, Phys. Rev. D **30**, 238 (1984).

[86] R. E. Peierls and J. Yoccoz, Proc. Phys. Soc. London Sect. A **70**, 381 (1957).

[87] X. M. Wang, X. T. Song, and P. C. Yin, Hadronic J. **6**, 985 (1983).

[88] X. D. Ji, Phys. Lett. B **254**, 456 (1991).

[89] C. Lorcé (private communication).

[90] M. von Laue, Ann. Phys. (Leipzig) **35**, 524 (1911); *Das Relativitätsprinzip* (Vieweg, Braunschweig, 1911).

[91] M. V. Polyakov and P. Schweitzer, in *Proceedings of "Photon 2019"*, Frascati Physics Series (2019), Vol. 69, p. 31.

[92] P. Hasenfratz and J. Kuti, Phys. Rep. **40**, 75 (1978).

[93] V. A. Novikov and M. A. Shifman, Z. Phys. C **8**, 43 (1981).

[94] M. B. Voloshin and V. I. Zakharov, Phys. Rev. Lett. **45**, 688 (1980).

[95] M. B. Voloshin and A. D. Dolgov, Yad. Fiz. **35**, 213 (1982) [Sov. J. Nucl. Phys. **35**, 120 (1982)].

[96] H. Leutwyler and M. A. Shifman, Phys. Lett. B **221**, 384 (1989).

[97] J. F. Donoghue and K. Johnson, Phys. Rev. D **21**, 1975 (1980).

[98] A. W. Thomas, Adv. Nucl. Phys. **13**, 1 (1984).

[99] V. D. Burkert and C. D. Roberts, Rev. Mod. Phys. **91**, 011003 (2019).

[100] B. L. G. Bakker, E. Leader, and T. L. Trueman, Phys. Rev. D **70**, 114001 (2004); E. Leader and C. Lorcé, Phys. Rep. **541**, 163 (2014).